Article

Journal of Vibration and Control
2015, Vol. 21(1) 157–180

DOI: 10.1177/1077546312472920
jvc.sagepub.com

Wave vibration control of planar frame structures based on the advanced Timoshenko bending theory

C Mei

Abstract

Coupled bending and axial vibrations in a planar multi-story frame structure are controlled from a wave vibration standpoint, in which vibrations are described as waves that propagate along uniform waveguides, and are reflected and transmitted upon structural discontinuities. The bending vibrations are modeled using a Timoshenko model, which takes into account the effects of rotary inertia and shear distortion. The axial vibrations are modeled using elementary theory, as it is typically valid for frequencies up to twice the cutoff frequency of Timoshenko bending waves. Regardless of the complexity of a structure, when it is modeled from a wave point of view, it consists of only two basic types of structural components, namely, structural elements and joints. In this paper, both structural element and structural joint controllers are designed based on various control strategies such as optimal damping and optimal energy absorbing. Numerical examples are presented. Results are compared to those obtained based on the classical Euler–Bernoulli model that are available in the literature. As was expected, good agreement between the results of the models at low frequencies was obtained.

Keywords

Timoshenko beam, wave vibration, vibration control, coupled motions, planar frame

Received: 24 July 2012; accepted: 7 November 2012

Introduction

In this paper, vibrations in multi-story planar frame structures are studied. Such structures can be found in many fields of engineering, and are often subject to harmful vibrations. Consequently, effective control of vibrations in these structures is of great importance.

Due to their complexity, vibrations in multi-story planar frame structures are often analyzed and controlled either based on approximated discrete models such as lumped mass/elasticity models, or using a numerical approach such as the finite-element analysis approach. Recently, the author developed a wave vibration analytical approach based on the classical Euler–Bernoulli model for analyzing and controlling vibrations in multi-story planar frame structures (Mei, 2011). From a wave vibration standpoint, vibrations are described as waves that propagate along a uniform waveguide (or structural element), and are reflected and transmitted at discontinuities (such as joints and boundaries) (Graff, 1975; Cremer et al., 1987; Doyle, 1989). Active 'discontinuities' are created either along structural elements or at structural joints to control the propagation, reflection, and transmission of an incident vibration wave.

Since the classical Euler–Bernoulli beam model considers only the lateral inertia and the elastic forces caused by bending deflections with the effects of rotary inertia and shear distortion neglected, the results obtained are only suitable for relatively low frequencies. At higher frequencies (typically when the transverse dimensions are not negligible with respect to the wavelength), the effects of rotary inertia and shear distortion must be taken into account. Rayleigh (1926) introduced the effect of rotatory inertia and Timoshenko (1921, 1922) extended it to include the effect of transverse shear deformation.

Department of Mechanical Engineering, The University of Michigan - Dearborn, USA

Corresponding author:
C Mei, Department of Mechanical Engineering, The University of Michigan - Dearborn, 4901 Evergreen Road, Dearborn, MI 48128, USA.
Email: cmei@umich.edu

Wave vibration control is normally feedforward, in which the disturbance is detected, and a control force applied somewhere downstream to produce a destructive signal to cancel the incoming wave or to absorb the energy associated with it (Von Flotow, 1985; Mace, 1987; Lu et al., 1989; Fuller et al., 1990; Clark et al., 1992; Elliott and Billet, 1993; Vipperman et al., 1993; Gardonio and Elliott, 1995). Wave control can also be feedback, and feedback controllers have been designed to control vibrations in beams (Elliott et al., 1993; Brennan, 1994; Mace and Jones, 1996; Mei et al., 2001; Mei, 2009).

In this paper, feedback wave control is designed to control coupled bending and axial vibrations in complex multi-story planar frame structures. The bending vibrations are modeled using advanced Timoshenko theory, and the axial waves are modeled by the elementary one-dimensional theory, which is typically valid for frequencies up to twice the cutoff frequency of Timoshenko bending waves (Wang and Rose, 2003).

This paper is organized as follows. In the next section, the equations for describing coupled bending and axial vibrations in a planar frame structure are presented. The propagation of waves along uniform structural elements and the reflection of waves at rolling, sliding, as well as classical boundaries are discussed. In section 3, controllers are designed for controlling the reflection and transmission characteristics of incoming vibration waves in a multi-story planar frame. These include both structural element and structural joint control. In section 4, expressions of waves generated by external disturbance forces as well as active control forces are derived. In section 5, numerical examples are presented, and conclusions are given in section 6.

2. Equations of motion, wave propagation, and wave reflection at boundaries

2.1. Equations of motion

The equations of motion for bending and longitudinal vibrations are (Ginsberg, 2001)

$$GA\kappa\left[\frac{\partial\psi(x,t)}{\partial x}-\frac{\partial^2 y(x,t)}{\partial x^2}\right]+\rho A\frac{\partial^2 y(x,t)}{\partial t^2}=q(x,t), \quad (1a)$$

$$EI\frac{\partial^2\psi(x,t)}{\partial x^2}+GA\kappa\left[\frac{\partial y(x,t)}{\partial x}-\psi(x,t)\right]-\rho I\frac{\partial^2\psi(x,t)}{\partial t^2}=0, \quad (1b)$$

$$\rho A\frac{\partial^2 u(x,t)}{\partial t^2}-EA\frac{\partial^2 u(x,t)}{\partial x^2}=p(x,t), \quad (1c)$$

where x is the position along the beam axis; t is time; $y(x,t)$ and $u(x,t)$ are the transverse and longitudinal deflection of the centerline of the beam; $q(x,t)$ and are $p(x,t)$ the externally applied transverse and longitudinal forces; and E, G, and ρ are the Young modulus, shear modulus, and mass density, respectively. I is the area moment of the inertia of the cross section; A is the cross-sectional area; κ is the shear coefficient; $\psi(x,t)$ is the slope due to bending; $\partial y(x,t)/\partial x$ is the slope of the centerline of the beam; and $\partial y(x,t)/\partial x-\psi(x,t)$ is the shear angle. Equation 1(a) and (b) are coupled through the slope and the transverse deflection of the structure.

The shear force $V(x,t)$, bending moment $M(x,t)$, and longitudinal force $F(x,t)$ at any section of the beam are related to the transverse deflection $y(x,t)$, the slope $\psi(x,t)$, and the longitudinal deflection $u(x,t)$ by

$$V(x,t)=GA\kappa\left[\frac{\partial y(x,t)}{\partial x}-\psi(x,t)\right], \quad (2)$$

$$M(x,t)=EI\frac{\partial\psi(x,t)}{\partial x}, \quad (3)$$

$$F(x,t)=EA\frac{\partial u(x,t)}{\partial x}. \quad (4)$$

2.2. Free wave propagation

2.2.1. Bending vibrations. First, consider the free bending vibration problem when no external force is applied to the beam. The differential equations of motion become

$$GA\kappa\left[\frac{\partial\psi(x,t)}{\partial x}-\frac{\partial^2 y(x,t)}{\partial x^2}\right]+\rho A\frac{\partial^2 y(x,t)}{\partial t^2}=0, \quad (5a)$$

$$EI\frac{\partial^2\psi(x,t)}{\partial x^2}+GA\kappa\left[\frac{\partial y(x,t)}{\partial x}-\psi(x,t)\right]-\rho I\frac{\partial^2\psi(x,t)}{\partial t^2}=0. \quad (5b)$$

Assuming time harmonic motion and using separation of variables, the solutions to equation (5) can be written in the form $y(x,t)=y(x)e^{-ikx}e^{i\omega t}$ and $\psi(x,t)=\psi(x)e^{-ikx}e^{i\omega t}$, where ω is the frequency and k the wavenumber. Substituting these expressions into equation (5) gives bending vibration wavenumbers that are functions of the frequency ω as well as the properties of the structure

$$k_1=\left\{\frac{1}{2}\left[\left(\frac{1}{C_s}\right)^2+\left(\frac{C_r}{C_b}\right)^2\right]\omega^2+\sqrt{\frac{\omega^2}{C_b^2}+\frac{1}{4}\left[\left(\frac{1}{C_s}\right)^2-\left(\frac{C_r}{C_b}\right)^2\right]^2\omega^4}\right\}^{\frac{1}{2}}, \quad (6a)$$

$$k_2 = \left\{ \left| \frac{1}{2}\left[\left(\frac{1}{C_s}\right)^2 + \left(\frac{C_r}{C_b}\right)^2 \right]\omega^2 - \sqrt{\frac{\omega^2}{C_b^2} + \frac{1}{4}\left[\left(\frac{1}{C_s}\right)^2 - \left(\frac{C_r}{C_b}\right)^2 \right]^2 \omega^4} \right| \right\}^{\frac{1}{2}}. \quad (6b)$$

where

$$C_b = \sqrt{\frac{EI}{\rho A}}, \quad C_s = \sqrt{\frac{GA\kappa}{\rho A}}, \quad \text{and } C_r = \sqrt{\frac{\rho I}{\rho A}}.$$

There exists a wave-mode transition at a cutoff frequency, which is given by

$$\omega_c = C_s/C_r. \quad (7)$$

Below the cutoff frequency, there exist a pair of propagating waves and a pair of decaying waves in the beam, while above the cutoff frequency, there are two pairs of propagating waves. In audio-frequency applications, the former case is overwhelmingly the most common.

Clearly, the wave amplitudes a of $y(x)$ and $\bar{a}$ of $\psi(x)$ are related to each other. The relation can be found from Equations (5) as

$$\begin{bmatrix} k^2 GA\kappa - \rho A\omega^2 & -ikGA\kappa \\ -ikGA\kappa & -k^2 EI - GA\kappa + \rho I\omega^2 \end{bmatrix} \begin{bmatrix} y \\ \psi \end{bmatrix} = 0. \quad (8)$$

from which

$$\frac{\psi}{y} = i\frac{\rho A\omega^2 - k^2 GA\kappa}{kGA\kappa} = i\frac{\omega^2 - k^2 C_s^2}{kC_s^2}. \quad (9)$$

Thus, the relations between the coefficients of $y(x)$ and those of $\psi(x)$ are

$$\frac{\overline{a_1^+}}{a_1^+} = -iP, \ \frac{\overline{a_1^-}}{a_1^-} = iP, \ \frac{\overline{a_2^+}}{a_2^+} = -N, \ \frac{\overline{a_2^-}}{a_2^-} = N, \quad (10)$$

where

$$P = k_1\left(1 - \frac{\omega^2}{k_1^2 C_s^2}\right), \quad \text{and } N = k_2\left(1 + \frac{\omega^2}{k_2^2 C_s^2}\right).$$

2.2.2. Longitudinal vibrations. Now consider the free longitudinal vibration problem when no external force is applied to the beam. The differential equation for free longitudinal motion is

$$\rho A\frac{\partial^2 u(x,t)}{\partial t^2} - EA\frac{\partial^2 u(x,t)}{\partial x^2} = 0 \quad (11)$$

Again assuming time harmonic motion and using separation of variables, the solution to equation (11) can be written in the form $u(x,t) = u_0 e^{-ikx} e^{i\omega t}$, where ω is the frequency and k the wavenumber. Substituting this into equation (11) gives the longitudinal wavenumber, which is

$$k_3 = \sqrt{\frac{\rho}{E}}\omega. \quad (12)$$

2.2.3. Propagation matrix. Two points A and B on a uniform beam a distance x apart are considered. Waves propagate from one point to the other, with the propagation being determined by the appropriate wavenumber. Denoting the positive and negative going wave vectors at points A and B as $\mathbf{a}^+$ and $\mathbf{a}^-$ and $\mathbf{b}^+$and $\mathbf{b}^-$, respectively, they are related by

$$\mathbf{a}^- = \mathbf{f}(x)\mathbf{b}^-; \quad \mathbf{b}^+ = \mathbf{f}(x)\mathbf{a}^+, \quad (13)$$

where

$$\mathbf{f}(x) = \begin{bmatrix} e^{-ik_1 x} & 0 & 0 \\ 0 & e^{-k_2 x} & 0 \\ 0 & 0 & e^{-ik_3 x} \end{bmatrix} \quad (14)$$

is the propagation matrix for a distance x. Furthermore

$$\mathbf{a}^+ = \begin{bmatrix} a_1^+ \\ a_2^+ \\ c^+ \end{bmatrix}, \quad \mathbf{a}^- = \begin{bmatrix} a_1^- \\ a_2^- \\ c^- \end{bmatrix}, \quad \mathbf{b}^+ = \begin{bmatrix} b_1^+ \\ b_2^+ \\ d^+ \end{bmatrix}, \quad \mathbf{b}^- = \begin{bmatrix} b_1^- \\ b_2^- \\ d^- \end{bmatrix}. \quad (15)$$

2.3. Reflections at boundaries

When an incident wave is reflected at a boundary, the incident wave $\mathbf{a}^+$ and the reflected wave $\mathbf{a}^-$ are related through the reflection matrix $\mathbf{r}$ by

$$\mathbf{a}^- = \mathbf{r}\mathbf{a}^+, \quad (16)$$

where $\mathbf{r}$ can be determined by considering equilibrium at the boundary.

Sliding and rolling boundaries are of interest when studying vibrations of planar frame structures. When a

frame is symmetrical about a vertical line through the centers of the spans, the vibration modes are either symmetrical or anti-symmetrical. It has been shown that vibrating in symmetrical modes, the mid-points of the cross-members behave as sliding ends; while vibrating in anti-symmetrical modes, the mid-points of the cross-members behave as rolling ends that are pinned vertically but allowing translational motion in the horizontal direction (Bishop and Johnson, 1960; Gladwell, 1964).

For a 'sliding' boundary, the equilibrium conditions at the boundary are

$$\psi = 0,\ V(x,t) = 0, \quad \text{and } u(x,t) = 0. \tag{17}$$

from which the reflection matrix is found as

$$\mathbf{r}_{sliding} = \begin{bmatrix} iP & N & 0 \\ ik_1 - iP & k_2 - N & 0 \\ 0 & 0 & 1 \end{bmatrix}^{-1} \begin{bmatrix} iP & N & 0 \\ ik_1 - iP & k_2 - N & 0 \\ 0 & 0 & -1 \end{bmatrix}. \tag{18}$$

The equilibrium conditions at the 'rolling' boundary are

$$y(x,t) = 0, \quad M(x,t) = 0, \text{ and } F(x,t) = 0. \tag{19}$$

The reflection matrix is

$$\mathbf{r}_{rolling} = \begin{bmatrix} -1 & -1 & 0 \\ k_1 P & -k_2 N & 0 \\ 0 & 0 & -ik_3 \end{bmatrix}^{-1} \begin{bmatrix} 1 & 1 & 0 \\ -k_1 P & k_2 N & 0 \\ 0 & 0 & -ik_3 \end{bmatrix}. \tag{20}$$

The reflection matrices at classical boundaries, that is, simply supported, clamped, and free boundaries are (Mei, 2008)

$$\mathbf{r}_s = \begin{bmatrix} -1 & 0 & 0 \\ 0 & -1 & 0 \\ 0 & 0 & -1 \end{bmatrix},$$
$$\mathbf{r}_c = \begin{bmatrix} \dfrac{P - iN}{P + iN} & \dfrac{-2iN}{P + iN} & 0 \\ \dfrac{-2P}{P + iN} & -\dfrac{P - iN}{P + iN} & 0 \\ 0 & 0 & -1 \end{bmatrix} \tag{21}$$

$$\mathbf{r}_f = \begin{bmatrix} \dfrac{-Pk_1(-N+k_2)+ik_2N(k_1-P)}{Pk_1(-N+k_2)+ik_2N(k_1-P)} & \dfrac{2Nk_2(-N+k_2)}{Pk_1(-N+k_2)+ik_2N(k_1-P)} & 0 \\ \dfrac{2iPk_1(-P+k_1)}{Pk_1(-N+k_2)+ik_2N(k_1-P)} & \dfrac{Pk_1(-N+k_2)-ik_2N(k_1-P)}{Pk_1(-N+k_2)+ik_2N(k_1-P)} & 0 \\ 0 & 0 & 1 \end{bmatrix}$$

3. Structural elements and structural joint control design

Regardless of the complexity of a structure, when it is modeled from a wave vibration point of view, it consists of only two basic types of structural components, namely, joints/supports and structural elements. As a result, vibrations can be controlled through controlling structural elements and/or joints/supports.

3.1. Structural element control

In wave control along a structural element, the reflection and transmission of waves are controlled using a collocated sensor and actuator, as shown in Figure 1(a). The wave control force F_c can be written in the frequency domain as

$$F_C = -H_w(\omega)w \tag{22}$$

where $H_w(\omega)$ is the frequency response of the controller. The control is dynamically identical to spring attachments, as shown in Figure 1(b). The dynamic translational and rotational stiffnesses are normally frequency dependent and complex.

The propagating wave incident upon a discontinuity will be partially transmitted and partially reflected.

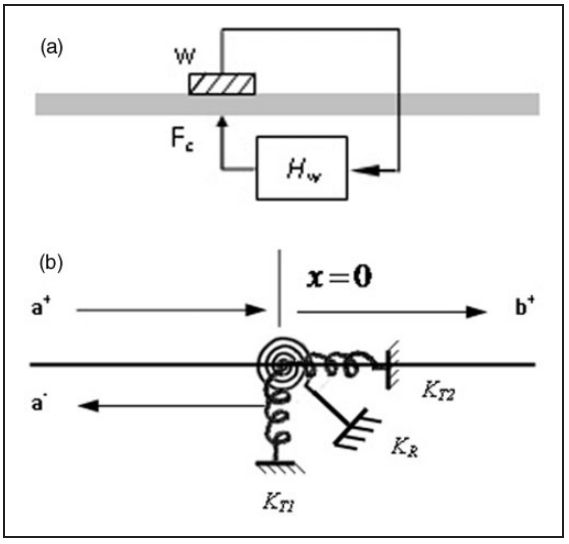

Figure 1. (a) Feedback control system and (b) wave scattering at a point support.

Denoting the incident propagating wave amplitudes as vector $\mathbf{a}^+$ the transmitted and reflected wave amplitudes $\mathbf{b}^-$ and $\mathbf{a}^-$ can then be found in terms of the transmission and reflection matrices $\mathbf{t}$ and $\mathbf{r}$ as

$$\mathbf{b}^+ = \mathbf{t}\mathbf{a}^+, \quad \mathbf{a}^- = \mathbf{r}\mathbf{a}^+ \tag{23}$$

The transmission and reflection matrices depend on the type of the discontinuity. For a given discontinuity, both the transmission and reflection matrices can be found through the particular equilibrium and continuity conditions, as mentioned earlier. The size of the vectors depends on the wave types and the number of wave components that exists in the structure.

Various control strategies can be adopted, such as absorbing the maximum amount of the energy carried by the incident waves, minimizing the transmitted vibration energy, or minimizing the reflected vibration energy, etc.

For example, an optimal damping controller that is designed to maximize the absorbed incoming bending vibration energy is found as (Mei, 2009)

$$K_{T1} = i\omega C(\omega) \tag{24a}$$

where

$$C(\omega) = \frac{2GA\kappa(-k_1 N + k_2 P)}{\omega\sqrt{P^2 + N^2}}.$$

A general optimal spring–damping controller for the same purpose, that is, maximizing the absorbed incoming bending vibration energy is (Mei, 2009)

$$K_{T1} = C_1(\omega) + i\omega C_2(\omega), \tag{24b}$$

where

$$C_1(\omega) = \frac{2GA\kappa P(k_1 N - k_2 P)}{P^2 + N^2} \text{ and}$$
$$C_2(\omega) = \frac{2GA\kappa N(k_1 N - k_2 P)}{\omega(P^2 + N^2)}.$$

An optimal damping controller that is designed to maximize the absorbed incoming longitudinal vibration energy is (Mei, 2002)

$$K_{T2} = i2\omega\sqrt{\rho E}A. \tag{24c}$$

A practical structure seldom consists of a single element. Structural elements are connected through various joints/supports to form a structure. Since vibration power flows from one element to another via structural joints/supports, active joints/supports are designed to control such vibration flow. A multi-story planar frame consists of two types of structural joints, namely, L- and T- joints. Joint control designs are considered as follows.

3.2. L-joint control

Wave transmission and reflection at an angle joint in general introduces wave mode conversion. For example, at an L-joint, an incident bending wave induces reflected and transmitted bending and axial waves in the members attached to the joint. This is evident from the coupled equilibrium and continuity relations below.

Figure 2 shows the free body diagram of an L-joint in planar motion. The equilibrium conditions are

$$\begin{aligned} F_2 - V_1 - K_T y_J &= m\ddot{y}_J, \\ -V_2 - F_1 - K_T u_J &= m\ddot{u}_J \\ M_2 - M_1 + V_1\frac{h_2}{2} + V_2\frac{h_1}{2} - K_R\psi_J &= J\ddot{\psi}_J \end{aligned} \tag{25}$$

where h is the beam thickness. Subscripts 1 and 2 refer to beam 1 and beam 2, and u_j, y_j and ψ_j are the displacements and rotation of the joint as indicated in the figure. The first two of these equations include the mass of the joint, while the third includes the moment of inertia of the joint and the moments induced by the off-set shear forces.

The continuity equations at the joint are

$$\begin{aligned} &u_1 = u_J,\ u_2 = y_J, \\ &y_1 = y_J - \frac{h_2}{2}\psi_J, \quad y_2 = -u_J + \frac{h_1}{2}\psi_J, \\ &\psi_1 = \psi_J,\ \psi_2 = \psi_J \end{aligned} \tag{26}$$

A set of positive going waves $\mathbf{a}^+$ incident upon the L-joint from one beam gives rise to transmitted and reflected waves $\mathbf{b}^+$ and $\mathbf{b}^-$, which are related to the incident waves through the transmission and reflection matrices $\mathbf{T}$ and $\mathbf{R}$ by

$$\mathbf{b}^+ = \mathbf{T}\mathbf{a}^+, \quad \mathbf{a}^- = \mathbf{R}\mathbf{a}^+ \tag{27}$$

Consider the general situation where beam 1 and 2 are of different materials and/or dimensions, and denote beam 1 and beam 2 related wavenumbers as $k_{1,2,3}$, and $k_{a,b,c}$, respectively, and the rest of beam 1 and beam 2 related physical parameters using subscripts 1 and 2. With an incident wave from beam 1, from the continuity conditions, one has

$$\begin{bmatrix} iP_2\frac{h_2}{2} & N_2\frac{h_2}{2} & 1 \\ 1 + iP_2\frac{h_1}{2} & 1 + N_2\frac{h_1}{2} & 0 \\ iP_2 & N_2 & 0 \end{bmatrix}\mathbf{b}^+ - \begin{bmatrix} 1 & 1 & 0 \\ 0 & 0 & -1 \\ -iP_1 & -N_1 & 0 \end{bmatrix}\mathbf{a}^- = \begin{bmatrix} 1 & 1 & 0 \\ 0 & 0 & -1 \\ iP_1 & N_1 & 0 \end{bmatrix}\mathbf{a}^+ \tag{28a}$$

The equilibrium conditions give

$$\begin{bmatrix} 0 & 0 & -ik_c(EA)_2+m\omega^2-K_{T1} \\ i(\kappa AG)_2(k_a-P_2) & (\kappa AG)_2(k_b-N_2) & 0 \\ -(EI)_2P_2k_a-i(\kappa AG)_2(k_a-P_2)\frac{h_1}{2} & (EI)_2N_2k_2-(\kappa AG)_2(k_b-N_2)\frac{h_1}{2} & 0 \\ -iP_2J\omega^2+iP_2K_R & -J\omega^2N_2+N_2K_R & \end{bmatrix}\mathbf{b}^+$$
$$-\begin{bmatrix} i(\kappa AG)_1(k_1-P_1) & (\kappa AG)_1(k_2-N_1) & 0 \\ 0 & 0 & -ik_3(EA)_1-m\omega^2+K_{T2} \\ -(EI)_1P_1k_1-i(\kappa AG)_1(k_1-P_1)\frac{h_2}{2} & (EI)_1N_1k_2-(\kappa AG)_1(k_2-N_1)\frac{h_2}{2} & 0 \end{bmatrix}\mathbf{a}^-$$
$$=\begin{bmatrix} -i(\kappa AG)_1(k_1-P_1) & -(\kappa AG)_1(k_2-N_1) & 0 \\ 0 & 0 & -ik_3(EA)_1-m\omega^2+K_{T2} \\ -(EI)_1P_1k_1+i(\kappa AG)_1(k_1-P_1)\frac{h_2}{2} & (EI)_1N_1k_2+(\kappa AG)_1(k_2-N_1)\frac{h_2}{2} & 0 \end{bmatrix}\mathbf{a}^+ \quad (28b)$$

The transmission and reflection matrices $\mathbf{T}_{12}$ and $\mathbf{R}_{11}$ can be obtained from solving equations (27), (28a), and (28b).

The transmission and reflection matrices $\mathbf{T}_{21}$ and $\mathbf{R}_{22}$ corresponding to an incident wave from beam 2 are obtained as

$$\begin{bmatrix} -iP_1\frac{h_1}{2} & -N_1\frac{h_1}{2} & 1 \\ 1+iP_1\frac{h_2}{2} & 1+N_1\frac{h_2}{2} & 0 \\ iP_1 & N_1 & 0 \end{bmatrix}\mathbf{b}^+-\begin{bmatrix} -1 & -1 & 0 \\ 0 & 0 & 1 \\ -iP_2 & -N_2 & 0 \end{bmatrix}\mathbf{a}^-$$
$$=\begin{bmatrix} -1 & -1 & 0 \\ 0 & 0 & 1 \\ iP_2 & N_2 & 0 \end{bmatrix}\mathbf{a}^+ \quad (29a)$$

$$\begin{bmatrix} 0 & 0 & ik_3(EA)_1-m\omega^2+K_{T1} \\ i(\kappa AG)_1(k_a-P_1) & (\kappa AG)_1(k_2-N_1) & 0 \\ -\left((EI)_1P_1k_1-i(\kappa AG)_1(k_1-P_1)\frac{h_2}{2}\right) & \left((EI)_1N_1k_2-(\kappa AG)_1(k_2-N_1)\frac{h_2}{2}\right) & 0 \\ -iP_1J\omega^2+iP_1K_R & -J\omega^2N_1+N_1K_R & \end{bmatrix}\mathbf{b}^+$$
$$-\begin{bmatrix} i(\kappa AG)_2(k_a-P_2) & (\kappa AG)_2(k_b-N_2) & 0 \\ 0 & 0 & -ik_c(EA)_2+m\omega^2-K_{T2} \\ -(EI)_2P_2k_a-i(\kappa AG)_2(k_a-P_2)\frac{h_1}{2} & (EI)_2N_2k_b-(\kappa AG)_2(k_b-N_2)\frac{h_1}{2} & 0 \end{bmatrix}\mathbf{a}^-$$
$$=\begin{bmatrix} -i(\kappa AG)_2(k_a-P_2) & -(\kappa AG)_2(k_b-N_2) & 0 \\ 0 & 0 & ik_c(EA)_2+m\omega^2-K_{T2} \\ -(EI)_2P_2k_a+i(\kappa AG)_2(k_a-P_2)\frac{h_1}{2} & (EI)_2N_2k_b+(\kappa AG)_2(k_b-N_2)\frac{h_1}{2} & 0 \end{bmatrix}\mathbf{a}^+ \quad (29b)$$

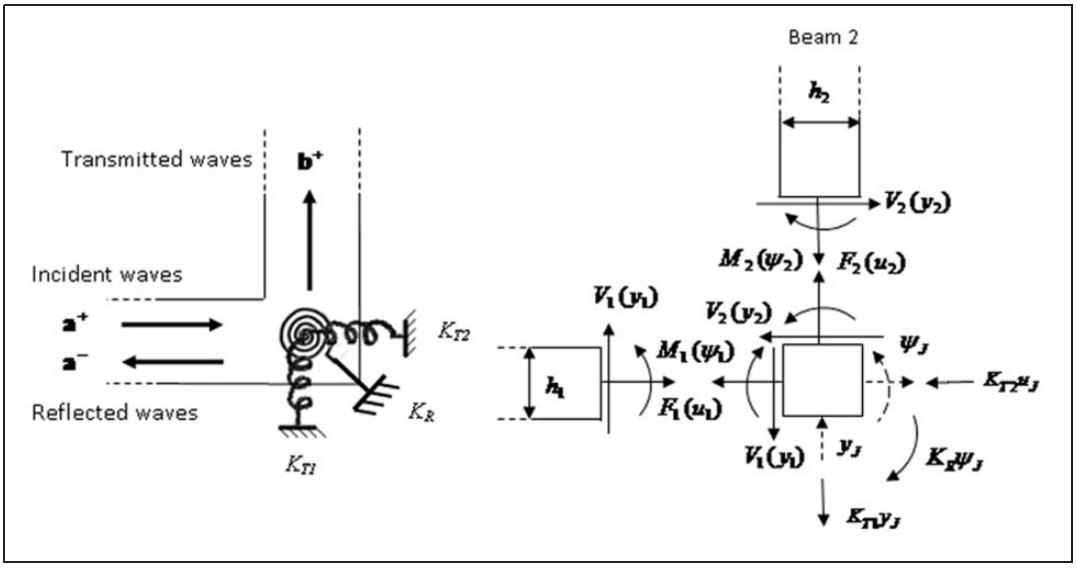

Figure 2. Free body diagram of an L-joint in planar motion.

3.3. T-Joint control

Similarly, wave transmission and reflection at a T-joint also introduce wave mode conversion. The transmission and reflection matrices are obtained by considering the continuity and equilibrium conditions at the joint. The free body diagram of a T-joint in planar motion is shown in Figure 3. The continuity equations at the joint are

$$u_1 = u_J,\ u_2 = y_J,\ u_3 = u_J,$$

$$y_1 = y_J - \frac{h_2}{2}\psi_J,\ y_2 = -u_J + \frac{h_1}{2}\psi_J,\ y_3 = y_J + \frac{h_3}{2}\psi_J,$$

$$\psi_1 = \psi_J,\ \psi_2 = \psi_J,\ \psi_3 = \psi_J \tag{30}$$

The equilibrium conditions are

$$V_3 + F_2 - V_1 - K_{T1} y_J = m\ddot{y}_J$$

$$F_3 - V_2 - F_1 - K_{T2} u_J = m\ddot{u}_J,$$

$$M_3 + M_2 - M_1 + V_3\frac{h_2}{2} + V_1\frac{h_2}{2} + V_2\frac{h_1}{2} - K_R\psi_J = J\ddot{\psi}_J \tag{31}$$

Consider again the general situation where beams 1, 2, and 3 are of different materials and/or dimensions, and denote beams 1, 2, and 3 related wavenumbers as $k_{1,2,3}$, $k_{a,b,c}$ and $k_{A,B,C}$ respectively, and the rest of beam 1, 2, and 3 related physical parameters using subscripts 1, 2, and 3.

There exist three sets of reflection and transmission relations, corresponding to incident waves from each of the three beam elements, respectively. First, let us consider waves incident from beam 1. The set of positive going incident waves $\mathbf{a}^+$ gives rise to reflected waves $\mathbf{a}^-$, and transmitted waves $\mathbf{b}^+$ and $\mathbf{e}^+$, which are related to the incident waves through the reflection and transmission matrices by

$$\mathbf{a}^- = r_{11}\mathbf{a}^+,\ \mathbf{b}^+ = t_{12}\mathbf{a}^+,\ \mathbf{e}^+ = t_{13}\mathbf{a}^+ \tag{32}$$

Wave vectors $\mathbf{a}^\pm$ and $\mathbf{b}^\pm$ are as defined in equation (15), and

$$\mathbf{e}^\pm = \begin{bmatrix} e_1^\pm \\ e_2^\pm \\ g^\pm \end{bmatrix} \tag{33}$$

With an incident wave from beam 1, from the continuity conditions, one has

$$\begin{bmatrix} iP_2\frac{h_2}{2} & N_2\frac{h_2}{2} & 1 \\ 1+iP_2\frac{h_1}{2} & 1+N_2\frac{h_1}{2} & 0 \\ iP_2 & N_2 & 0 \end{bmatrix}\mathbf{b}^+ - \begin{bmatrix} 1 & 1 & 0 \\ 0 & 0 & -1 \\ -iP_1 & -N_1 & 0 \end{bmatrix}\mathbf{a}^- = \begin{bmatrix} 1 & 1 & 0 \\ 0 & 0 & -1 \\ iP_1 & N_1 & 0 \end{bmatrix}\mathbf{a}^+ \tag{34}$$

and

$$\begin{bmatrix} 1+iP_3\dfrac{h_2+h_3}{2} & 1+N_3\dfrac{h_2+h_3}{2} & 0 \\ 0 & 0 & 1 \\ iP_3 & N_3 & 0 \end{bmatrix}\mathbf{e}^+ - \begin{bmatrix} 1 & 1 & 0 \\ 0 & 0 & 1 \\ -iP_1 & -N_1 & 0 \end{bmatrix}\mathbf{a}^- = \begin{bmatrix} 1 & 1 & 0 \\ 0 & 0 & 1 \\ iP_1 & N_1 & 0 \end{bmatrix}\mathbf{a}^+. \tag{35}$$

The equilibrium conditions give

$$\mathbf{E}_{t13}\mathbf{e}^+ + \mathbf{E}_{t12}\mathbf{b}^+ - \mathbf{E}_{r11}\mathbf{a}^- = \mathbf{E}_1\mathbf{a}^+ \tag{36}$$

where

$$\mathbf{E}_{t13} = \begin{bmatrix} -(GA\kappa)_3(-ik_A+iP_3) & -(AG\kappa)_3(-k_B+N_3) & 0 \\ 0 & 0 & (EA)_3ik_c \\ -(EI)_3P_3k_A+\frac{h_2}{2}(\kappa AG)_3(-ik_A+iP_3) & (EI)_3N_3k_B+\frac{h_2}{2}(\kappa AG)_3(-k_B+N_3) & 0 \end{bmatrix}$$

$$\mathbf{E}_{t12} = \begin{bmatrix} 0 & 0 & (EA)_2ik_c-m\omega^2+K_{T1} \\ (\kappa AG)_2(-ik_a+iP_2) & (\kappa AG)_2(-k_b+N_2) & 0 \\ \begin{pmatrix} -(EI)_2P_2k_a+\frac{h_1}{2}(\kappa AG)_2 \\ (-ik_a+iP_2)-J\omega^2iP_2+K_RiP_2 \end{pmatrix} & \begin{pmatrix} (EI)_2N_2k_b+\frac{h_1}{2}(\kappa AG)_2 \\ (-k_b+N_2)-J\omega^2N_2+K_RN_2 \end{pmatrix} & 0 \end{bmatrix}$$

$$\mathbf{E}_{r11} = \begin{bmatrix} (\kappa AG)_1(-ik_1+iP_1) & (\kappa AG)_1(-k_2+N_1) & 0 \\ 0 & 0 & -(EA)_1ik_3+m\omega^2-K_{T2} \\ -(EI)_1P_1k_1-\frac{h_2}{2}(\kappa AG)_1(ik_1-iP_1) & (EI)_1N_1k_2-\frac{h_2}{2}(\kappa AG)_1(k_2-N_1) & 0 \end{bmatrix}$$

$$\mathbf{E}_1 = \begin{bmatrix} (\kappa AG)_1(ik_1-iP_1) & (\kappa AG)_1(k_2-N_1) & 0 \\ 0 & 0 & (EA)_1ik_3+m\omega^2-K_{T2} \\ -(EI)_1P_1k_1+\frac{h_2}{2}(\kappa AG)_1(ik_1-iP_1) & (EI)_1N_1k_2+\frac{h_2}{2}(\kappa AG)_1(k_2-N_1) & 0 \end{bmatrix}$$

The reflection and transmission matrices $\mathbf{r}_{11}$, $\mathbf{t}_{12}$, and $\mathbf{t}_{13}$ can be obtained from equations (32), (34), (35), and (36).

Consider waves incident from beam 3. Incident waves $\mathbf{a}^+$ give rise to reflected waves $\mathbf{a}^-$, and transmitted waves $\mathbf{b}^+$ and $\mathbf{e}^+$, which are related to the incident waves through the reflection and transmission matrices by

$$\mathbf{a}^- = \mathbf{r}_{33}\mathbf{a}^+, \quad \mathbf{b}^+ = \mathbf{t}_{32}\mathbf{a}^+, \quad \mathbf{e}^+ = \mathbf{t}_{31}\mathbf{a}^+. \tag{37}$$

Following a similar procedure, one obtains two continuity conditions and one equilibrium condition related equations

$$\begin{bmatrix} -iP_2\dfrac{h_3}{2} & -N_2\dfrac{h_3}{2} & 1 \\ -1-iP_2\dfrac{h_1}{2} & -1-N_2\dfrac{h_1}{2} & 0 \\ -iP_2 & -N_2 & 0 \end{bmatrix}\mathbf{t}_{32} - \begin{bmatrix} 1 & 1 & 0 \\ 0 & 0 & 1 \\ -iP_3 & -N_3 & 0 \end{bmatrix}\mathbf{r}_{33} = \begin{bmatrix} 1 & 1 & 0 \\ 0 & 0 & 1 \\ iP_3 & N_3 & 0 \end{bmatrix},$$

$$\begin{bmatrix} 1+iP_1\dfrac{h_2+h_3}{2} & 1+N_1\dfrac{h_2+h_3}{2} & 0 \\ 0 & 0 & 1 \\ iP_1 & N_1 & 0 \end{bmatrix}\mathbf{t}_{31} - \begin{bmatrix} 1 & 1 & 0 \\ 0 & 0 & 1 \\ -iP_3 & -N_3 & 0 \end{bmatrix}\mathbf{r}_{33} = \begin{bmatrix} 1 & 1 & 0 \\ 0 & 0 & 1 \\ iP_3 & N_3 & 0 \end{bmatrix} \tag{38}$$

$$\mathbf{D}_{t_{31}}\mathbf{t}_{31} + \mathbf{D}_{t_{32}}\mathbf{t}_{32} - \mathbf{D}_{r_{33}}\mathbf{r}_{33} = \mathbf{D}_3$$

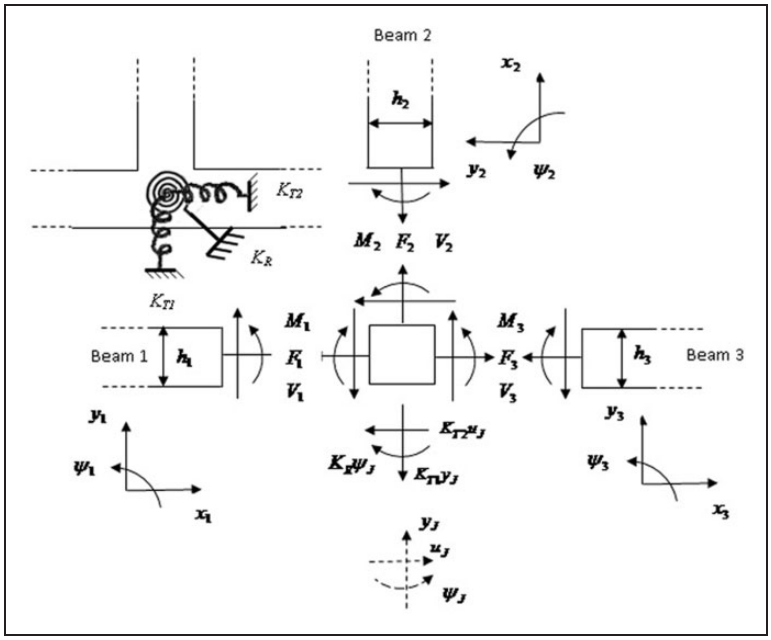

Figure 3. Free body diagram of a T-joint in planar motion.

where

$$\mathbf{D}_{t_{31}} = \begin{bmatrix} (\kappa AG)_1(ik_1 - iP_1) & (\kappa AG)_1(k_2 - N_1) & 0 \\ 0 & 0 & (EA)_1 ik_3 - m\omega^2 + K_{T2} \\ (EI)_1 P_1 k_1 + \dfrac{h_2}{2}(\kappa AG)_1(ik_1 - iP_1) & -(EI)_1 N_1 k_2 + \dfrac{h_2}{2}(\kappa AG)_1(k_2 - N_1) & 0 \end{bmatrix}$$

$$\mathbf{D}_{t_{32}} = \begin{bmatrix} 0 & 0 & (EA)_2 ik_c - m\omega^2 + K_{T1} \\ (\kappa AG)_2(-ik_a + iP_2) & (\kappa AG)_2(-k_b + N_2) & 0 \\ \begin{pmatrix} -(EI)_2 P_2 k_a + \dfrac{h_1}{2}(\kappa AG)_2 \\ (-ik_a + iP_2) - J\omega^2 iP_2 + K_R iP_2 \end{pmatrix} & \begin{pmatrix} (EI)_2 N_2 k_b + \dfrac{h_1}{2}(\kappa AG)_2 \\ (-k_b + N_2) - J\omega^2 N_2 + K_R N_2 \end{pmatrix} & 0 \end{bmatrix}$$

$$\mathbf{D}_{r_{33}} = \begin{bmatrix} (\kappa AG)_3(-ik_A + iP_3) & (\kappa AG)_3(-k_B + N_3) & 0 \\ 0 & 0 & -(EA)_3 ik_C \\ (EI)_3 P_3 k_A + \dfrac{h_2}{2}(\kappa AG)_3(ik_A - iP_3) & -(EI)_3 N_3 k_B + \dfrac{h_2}{2}(\kappa AG)_3(k_B - N_3) & 0 \end{bmatrix}$$

$$\mathbf{D}_3 = \begin{bmatrix} (\kappa AG)_3(ik_A - iP_3) & (\kappa AG)_3(k_B - N_3) & 0 \\ 0 & 0 & (EA)_3 ik_C \\ (EI)_3 P_3 k_A - \dfrac{h_2}{2}(\kappa AG)_3(ik_A - iP_3) & -(EI)_3 N_3 k_B - \dfrac{h_2}{2}(\kappa AG)_3(k_B - N_3) & 0 \end{bmatrix}$$

The reflection and transmission matrices $\mathbf{r}_{33}$, $\mathbf{t}_{31}$, and $\mathbf{t}_{32}$ can be obtained from solving equation (38).

Lastly, consider waves incident from beam 2. Incident waves $\mathbf{a}^+$ give rise to reflected waves $\mathbf{a}^-$, and transmitted waves $\mathbf{b}^+$ and $\mathbf{e}^+$, which are related to the incident waves through the reflection and transmission matrices by

$$\mathbf{a}^- = \mathbf{r}_{22}\mathbf{a}^+,\ \mathbf{b}^+ = \mathbf{t}_{23}\mathbf{a}^+,\ \mathbf{e}^+ = \mathbf{t}_{21}\mathbf{a}^+. \qquad (39)$$

Again, following a similar procedure, one obtains two continuity conditions and one equilibrium condition related equations

$$\begin{bmatrix} 1+iP_1\frac{h_2}{2} & 1+N_1\frac{h_2}{2} & 0 \\ iP_1\frac{h_1}{2} & N_1\frac{h_1}{2} & -1 \\ iP_1 & N_1 & 0 \end{bmatrix}\mathbf{t}_{21} - \begin{bmatrix} 0 & 0 & 1 \\ 1 & 1 & 0 \\ -iP_2 & -N_2 & 0 \end{bmatrix}\mathbf{r}_{22} = \begin{bmatrix} 0 & 0 & 1 \\ 1 & 1 & 0 \\ iP_2 & N_2 & 0 \end{bmatrix}$$

$$\begin{bmatrix} 1+iP_3\frac{h_3}{2} & 1+N_3\frac{h_3}{2} & 0 \\ -iP_3\frac{h_1}{2} & -N_3\frac{h_1}{2} & -1 \\ -iP_3 & -N_3 & 0 \end{bmatrix}\mathbf{t}_{23} - \begin{bmatrix} 0 & 0 & 1 \\ 1 & 1 & 0 \\ -iP_2 & -N_2 & 0 \end{bmatrix}\mathbf{r}_{22} = \begin{bmatrix} 0 & 0 & 1 \\ 1 & 1 & 0 \\ iP_2 & N_2 & 0 \end{bmatrix}, \quad (40)$$

$$\mathbf{C}_{t_{21}}\mathbf{t}_{21} + \mathbf{C}_{t_{23}}\mathbf{t}_{23} - \mathbf{C}_{r_{22}}\mathbf{r}_{22} = \mathbf{C}_2$$

where

$$\mathbf{C}_{t_{21}} = \begin{bmatrix} (\kappa AG)_1(ik_1 - iP_1) & (\kappa AG)_1(k_2 - N_1) & 0 \\ 0 & 0 & (EA)_1 ik_3 - m\omega^2 + K_{T2} \\ \begin{pmatrix} (EI)_1 P_1 k_1 + \frac{h_2}{2}(\kappa AG)_1 \\ (ik_1 - iP_1) + J\omega^2 iP_1 - K_R iP_1 \end{pmatrix} & \begin{pmatrix} -(EI)_1 N_1 k_2 + \frac{h_2}{2}(\kappa AG)_1 \\ (k_2 - N_1) + J\omega^2 N_1 - K_R N_1 \end{pmatrix} & 0 \end{bmatrix}$$

$$\mathbf{C}_{t_{23}} = \begin{bmatrix} (\kappa AG)_3(ik_A - iP_3) & (\kappa AG)_3(k_B - N_3) & 0 \\ 0 & 0 & (EA)_3 ik_C \\ -(EI)_3 P_3 k_A + \frac{h_2}{2}(\kappa AG)_3(-ik_A + iP_3) & (EI)_3 N_3 k_B + \frac{h_2}{2}(\kappa AG)_3(-k_B + N_3) & 0 \end{bmatrix}$$

$$\mathbf{C}_{r_{22}} = \begin{bmatrix} 0 & 0 & -(EA)_2 ik_c + m\omega^2 - K_{T1} \\ (\kappa AG)_2(ik_a - iP_2) & (\kappa AG)_2(k_b - N_2) & 0 \\ (EI)_2 P_2 k_a + \frac{h_1}{2}(\kappa AG)_2(ik_a - iP_2) & -(EI)_2 N_2 k_b + \frac{h_1}{2}(\kappa AG)_2(k_b - N_2) & 0 \end{bmatrix}$$

$$\mathbf{C}_2 = \begin{bmatrix} 0 & 0 & (EA)_2 ik_c + m\omega^2 - K_{T1} \\ -(\kappa AG)_2(ik_a - iP_2) & -(\kappa AG)_2(k_b - N_2) & 0 \\ (EI)_2 P_2 k_a - \frac{h_1}{2}(\kappa AG)_2(ik_a - iP_2) & -(EI)_2 N_2 k_b - \frac{h_1}{2}(\kappa AG)_2(k_b - N_2) & 0 \end{bmatrix}$$

The reflection and transmission matrices $\mathbf{r}_{22}$, $\mathbf{t}_{21}$, and $\mathbf{t}_{23}$ can be obtained by solving equation (40).

It is evident that the reflection and transmission coefficients are dependent on the point attachments and parameters K_{T1}, K_{T2}, and K_R of the point discontinuity, and can be designed to control the vibration flow through the L- and T-joints.

4. Waves generated by external forces

4.1. Disturbance force

Waves generated by externally applied point forces and moments (see Figure 4) can also be found by considering the continuity and equilibrium conditions at the external force/moment applied point (Mei, 2008)

$$\mathbf{b}^+ - \mathbf{a}^+ = \mathbf{q} + \mathbf{m} - \mathbf{f}, \quad \mathbf{b}^- - \mathbf{a}^- = -\mathbf{q} + \mathbf{m} + \mathbf{f}, \quad (41)$$

where the vectors of the excited wave amplitudes are

$$\mathbf{q} = \begin{bmatrix} iN \\ P \\ 0 \end{bmatrix}\frac{\bar{Q}}{2GA\kappa(k_2 P - k_1 N)}, \quad (42)$$

$$\mathbf{m} = \begin{bmatrix} 1 \\ -1 \\ 0 \end{bmatrix}\frac{\bar{M}}{2EI(k_1 P + k_2 N)}, \ \mathbf{f} = \begin{bmatrix} 0 \\ 0 \\ i \end{bmatrix}\frac{\bar{F}}{2EAk_3}.$$

4.2. Control force

The propagating wave incident upon the control force induced discontinuity (see Figure 1) is partially transmitted and partially reflected. Denoting the incident propagating wave amplitudes as vector $\mathbf{a}^+$, the transmitted and reflected wave amplitudes $\mathbf{b}^+$ and $\mathbf{a}^-$ can

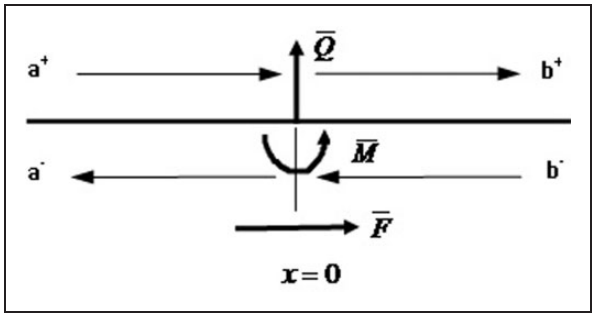

Figure 4. Waves generated by externally applied point forces and moments.

then be found in terms of the transmission and reflection matrices $\mathbf{t}$ and $\mathbf{r}$ as

$$\mathbf{b}^+ = \mathbf{t}_c\mathbf{a}^+, \quad \mathbf{a}^- = \mathbf{r}_c\mathbf{a}^+ \tag{43}$$

where $\mathbf{r}_c$ and $\mathbf{t}_c$ are the control force related reflection and transmission matrices. The reflection and transmission at a control force applied point are found by considering the continuity and equilibrium conditions as

$$\begin{bmatrix} 1 & 1 & 0 \\ iP & N & 0 \\ 0 & 0 & 1 \end{bmatrix}\mathbf{b}^+ - \begin{bmatrix} 1 & 1 & 0 \\ -iP & -N & 0 \\ 0 & 0 & 1 \end{bmatrix}\mathbf{a}^- = \begin{bmatrix} 1 & 1 & 0 \\ iP & N & 0 \\ 0 & 0 & 1 \end{bmatrix}\mathbf{a}^+$$

$$\begin{bmatrix} ik_1 + K_{T1}/(GA\kappa) & k_2 + K_{T1}/(GA\kappa) & 0 \\ -k_1P - iPK_R/(EI) & k_2N - NK_R/(EI) & 0 \\ 0 & 0 & i + K_{T2}/(EAk_3) \end{bmatrix}\mathbf{b}^+$$

$$-\begin{bmatrix} -ik_1 & -k_2 & 0 \\ -k_1P & k_2N & 0 \\ 0 & 0 & -i \end{bmatrix}\mathbf{a}^- = \begin{bmatrix} ik_1 & k_2 & 0 \\ -k_1P & k_2N & 0 \\ 0 & 0 & i \end{bmatrix}\mathbf{a}^+ \tag{44}$$

The control force related reflection and transmission matrices $\mathbf{r}_c$ and $\mathbf{t}_c$ can then be solved from equations (43) and (44).

5. Control of vibrations in multi-story frames

The same multi-story frame that is symmetrical about a vertical line through the centers of the spans, as considered in Mei (2011), is studied. As shown in Figure 5, an external excitation force G is applied at a point that is L_{11} distance away from the boundary. An element control force F_E is applied at a point $L_{11} + L_{22}$ distance away from the boundary. There exist several discontinuities in the frame, namely, the L- and T-joints (with or without the joint control forces F_L and F_T), the boundaries, the application point of the disturbance force G and the element control force F_E. The propagation, reflection, and transmission relations in the planar frame are as follows.

- The three pairs of propagation relations on the beam element where external disturbance force G and element control force F_E are applied are

$$\begin{aligned} \mathbf{g}_{11}^+ &= \mathbf{f}(L_{11})\mathbf{A}_0^+, \quad \mathbf{A}_0^- = \mathbf{f}(L_{11})\mathbf{g}_{11}^-; \\ \mathbf{f}_{22}^+ &= \mathbf{f}(L_{22})\mathbf{g}_{12}^+, \quad \mathbf{g}_{12}^- = \mathbf{f}(L_{22})\mathbf{f}_{22}^-; \\ \mathbf{a}_1^+ &= \mathbf{f}(L_{33})\mathbf{f}_{23}^+, \quad \mathbf{f}_{23}^- = \mathbf{f}(L_{33})\mathbf{a}_1^-. \end{aligned} \tag{45a}$$

- The n pairs of propagation relations along the rest of the uniform vertical beam elements are

$$\mathbf{a}_i^+ = \mathbf{f}(L)\mathbf{A}_{i-1}^+, \ \mathbf{A}_{i-1}^- = \mathbf{f}(L)\mathbf{a}_i^-, \ \text{where } i = 1, 2, \ldots, n. \tag{45b}$$

- The n pairs of propagation relations along the uniform horizontal beam elements are

$$\mathbf{c}_{Ri}^+ = \mathbf{f}(L_H/2)\mathbf{c}_{Li}^+, \ \mathbf{c}_{Li}^- = \mathbf{f}(L_H/2)\mathbf{c}_{Ri}^-, \ \text{where } i = 1, 2, \ldots, n. \tag{45c}$$

- The reflection and transmission relations of the waves at the 'T' joints are

$$\begin{aligned} \mathbf{a}_i^- &= \mathbf{r}_{11}\mathbf{a}_i^+ + \mathbf{t}_{31}\mathbf{A}_i^- + \mathbf{t}_{21}\mathbf{c}_{Li}^-, \\ \mathbf{A}_i^+ &= \mathbf{r}_{33}\mathbf{A}_i^- + \mathbf{t}_{13}\mathbf{a}_i^+ + \mathbf{t}_{23}\mathbf{c}_{Li}^-, \\ \mathbf{c}_{Li}^+ &= \mathbf{r}_{22}\mathbf{c}_{Li}^- + \mathbf{t}_{12}\mathbf{a}_i^+ + \mathbf{t}_{32}\mathbf{A}_i^-, \ \text{where } i = 1, 2, \ldots, n-1 \end{aligned} \tag{45d}$$

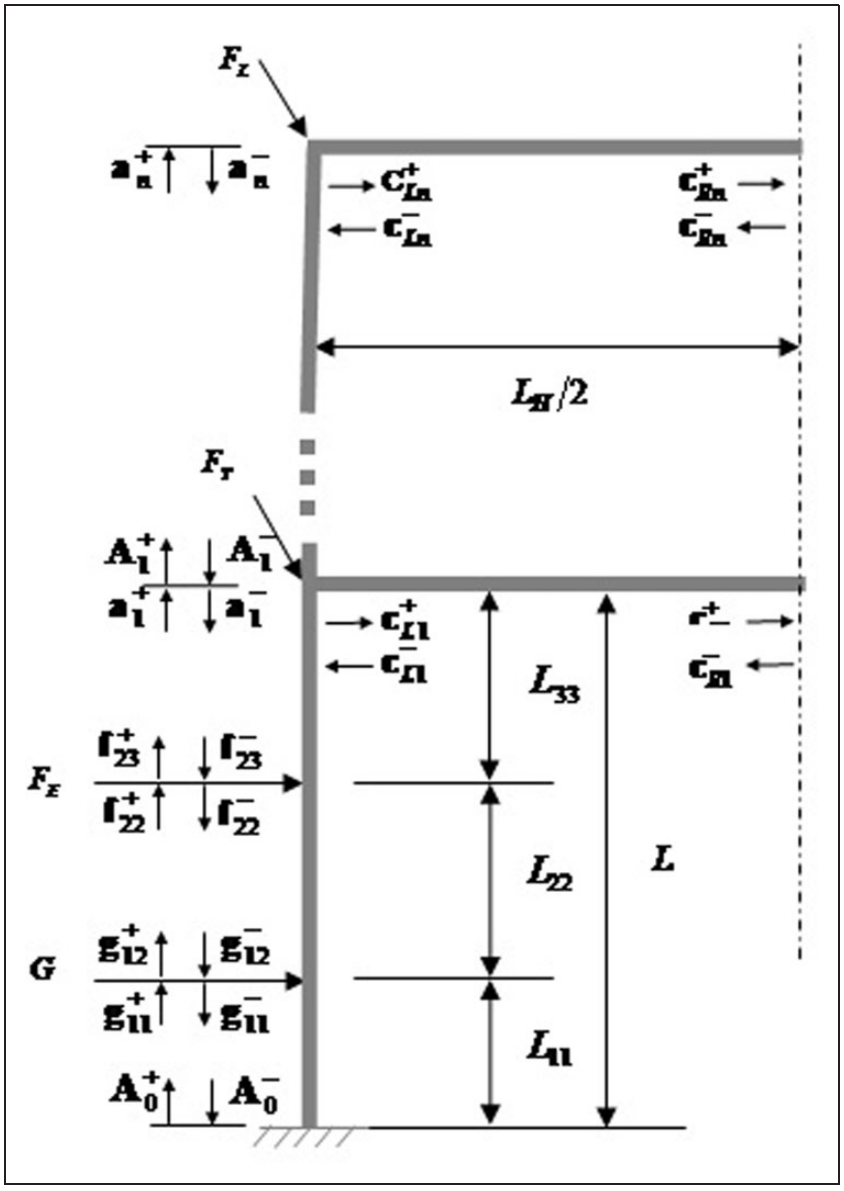

Figure 5. Structural element and joint control of a multi-story frame.

- The reflection and transmission relations of the waves at the 'L' joint are

$$\mathbf{c}_{Ln}^{+} = \mathbf{R}_{22}\mathbf{c}_{Ln}^{-} + \mathbf{T}_{12}\mathbf{a}_{n}^{+},\ \mathbf{a}_{n}^{-} = \mathbf{R}_{11}\mathbf{a}_{n}^{+} + \mathbf{T}_{21}\mathbf{c}_{Ln}^{-}. \tag{45e}$$

- The reflection relations at the sliding/rolling boundaries are

$$\mathbf{c}_{Ri}^{-} = \mathbf{r}_{sliding/rolling}\mathbf{c}_{Ri}^{+}, \quad \text{where } i = 1, 2, \ldots, n. \tag{45f}$$

- The reflection at the classical boundary is

$$\mathbf{A}_{0}^{+} = \mathbf{r}_{0}\mathbf{A}_{0}^{-}. \tag{45g}$$

- At the application point of the disturbance force G

$$\mathbf{g}_{12}^{+} - \mathbf{g}_{11}^{+} = \mathbf{q} + \mathbf{m} - \mathbf{f},\ \mathbf{g}_{12}^{-} - \mathbf{g}_{11}^{-} = -\mathbf{q} + \mathbf{m} + \mathbf{f} \tag{45h}$$

- At the application point of the control force F_E

$$\mathbf{f}_{22}^{-} = \mathbf{r}_{c}\mathbf{f}_{22}^{+} + \mathbf{t}_{c}\mathbf{f}_{23}^{-}, \quad \mathbf{f}_{23}^{+} = \mathbf{r}_{c}\mathbf{f}_{23}^{-} + \mathbf{t}_{c}\mathbf{f}_{22}^{+} \tag{45i}$$

Assembling these propagation, reflection, and transmission relations allows one to find the forced vibrations. In matrix form

$$\mathbf{A}_{f}\mathbf{z}_{f} = \mathbf{F} \tag{46}$$

where $\mathbf{A}_f$ is a square coefficient matrix, $\mathbf{z}_f$ is a wave component vector, and $\mathbf{F}$ is a vector describing the externally applied forces and moments.

The deflection of any point in the frame can then be found. For example, the deflection at a point on the vertical leg between forces G and F that is x_1 distance away from the boundary is given by

$$y_1 = \begin{bmatrix} 1 & 1 & 1 \end{bmatrix} \mathbf{f}(x_1 - L_{11})\mathbf{g}_{12}^{+} + \begin{bmatrix} 1 & 1 & 1 \end{bmatrix} \times \mathbf{f}(-(x_1 - L_{11}))\mathbf{g}_{12}^{-} \quad (47a)$$

Similarly, the deflection at a point on the ith horizontal beam that is x_1 distance away from the ith joint is

$$y_2 = \begin{bmatrix} 1 & 1 & 1 \end{bmatrix} \mathbf{f}(x_2)\mathbf{c}_{Li}^{+} + \begin{bmatrix} 1 & 1 & 1 \end{bmatrix} \mathbf{f}(-x_2))\mathbf{c}_{Li}^{-} \quad (47b)$$

As an example, let us take a look at the control of vibrations in the same two-story frame studied by (Petyt, 1990; Mei, 2011). The lengths of vertical and horizontal beams are $L = 22.86\,\text{cm}$ and $L_H = 45.72\,\text{cm}$, respectively, the cross section of the beam elements is $0.3175 \times 1.27\,\text{cm}^2$, Young's modulus E is $206.84\,\text{GN/m}^2$, and the mass density ρ is $7830\,\text{kg/m}^3$. The boundary conditions are clamped–clamped. Poisson's ratio $\nu = 0.29$, the shear modulus is calculated using

$$G = \frac{E}{2(1+\nu)}$$

and the shear coefficient κ is found from

$$\kappa = \frac{10(1+\nu)}{12+11\nu}$$

(Cowper, 1966). Boundary conditions are assumed clamped. The responses are measured at two locations: location 1 (x_1) is in between forces G and F; location 2 (x_2) is on the top horizontal bar. In the numerical example, the parameters are chosen as: $L_{11} = 0.38L$, $L_{11} + L_{22} = 0.68L$, $x_1 = 0.52L$, and $x_2 = 0.35L_H$.

5.1. Timoshenko and Euler–Bernoulli bending theories

Before applying control, the receptance frequency responses of the example multi-story frame using Timoshenko and Euler–Bernoulli bending theories were obtained. Figures 6 to 8 show the receptance frequency responses subject to a point transverse force, a point longitudinal force, and a bending moment excitation, respectively. It can be seen that good agreements are reached at low frequencies. However, the discrepancies at higher frequencies are significant. This finding agrees with those observations from simple beam elements, that is, when the transverse dimensions are not negligible with respect to the wavelength, the effects of rotary inertia and shear distortion must be taken into account.

Figure 9 shows the magnitude responses of the characteristic polynomial of the multi-story planar frame based on Timoshenko and Euler–Bernoulli bending theories. The frequency readings at zero magnitude are the natural frequencies of the frame. It can be seen that regardless of whether the frame vibrates at symmetrical or anti-symmetrical modes, at higher frequencies, the predicted natural frequencies based on Timoshenko theory are less than those from Euler–Bernoulli bending theory. This again agrees with the observations of simple beam elements.

The above analysis addresses the importance of taking into account the effects of rotary inertia and shear distortion when the transverse dimensions are not negligible with respect to the wavelength. In the studies that follow, Timoshenko bending theory is adopted for bending vibration, and elementary theory is used for axial vibration. The cutoff frequency for in-plane bending vibration of this example structure is found from equation (7) as 512 kHz. The maximum frequency considered in this study is 12 kHz, which justifies the adoption of the elementary theory for axial vibration analysis, as it is valid up to twice the cutoff bending frequency according to Wang and Rose (2003).

5.2. Structural element control

Figure 10 shows the receptance frequency responses of the example multi-story frame before and after structural element control subject to a point transverse force. In the control design, K_R is set to zero, and K_{T1} and K_{T2} are designed to optimally damp out the flexural and longitudinal vibration energy, respectively. For simplicity, the excitation is assumed to be a point transverse force. It can be seen that the optimally designed controller adds damping to the structure, and the resonant peaks are much less sharp after control.

5.3. L-joint control

In the L-joint control design, K_{T1} and K_{T2} are set to zero, and K_R is designed to damp out optimally the reflected bending and longitudinal vibration energies. Figure 11 shows the receptance frequency responses of the frame before and after control.

5.4. T-joint control

In the T-joint control design, K_{T1} and K_{T2} are set to zero, and K_R is designed to damp out optimally the

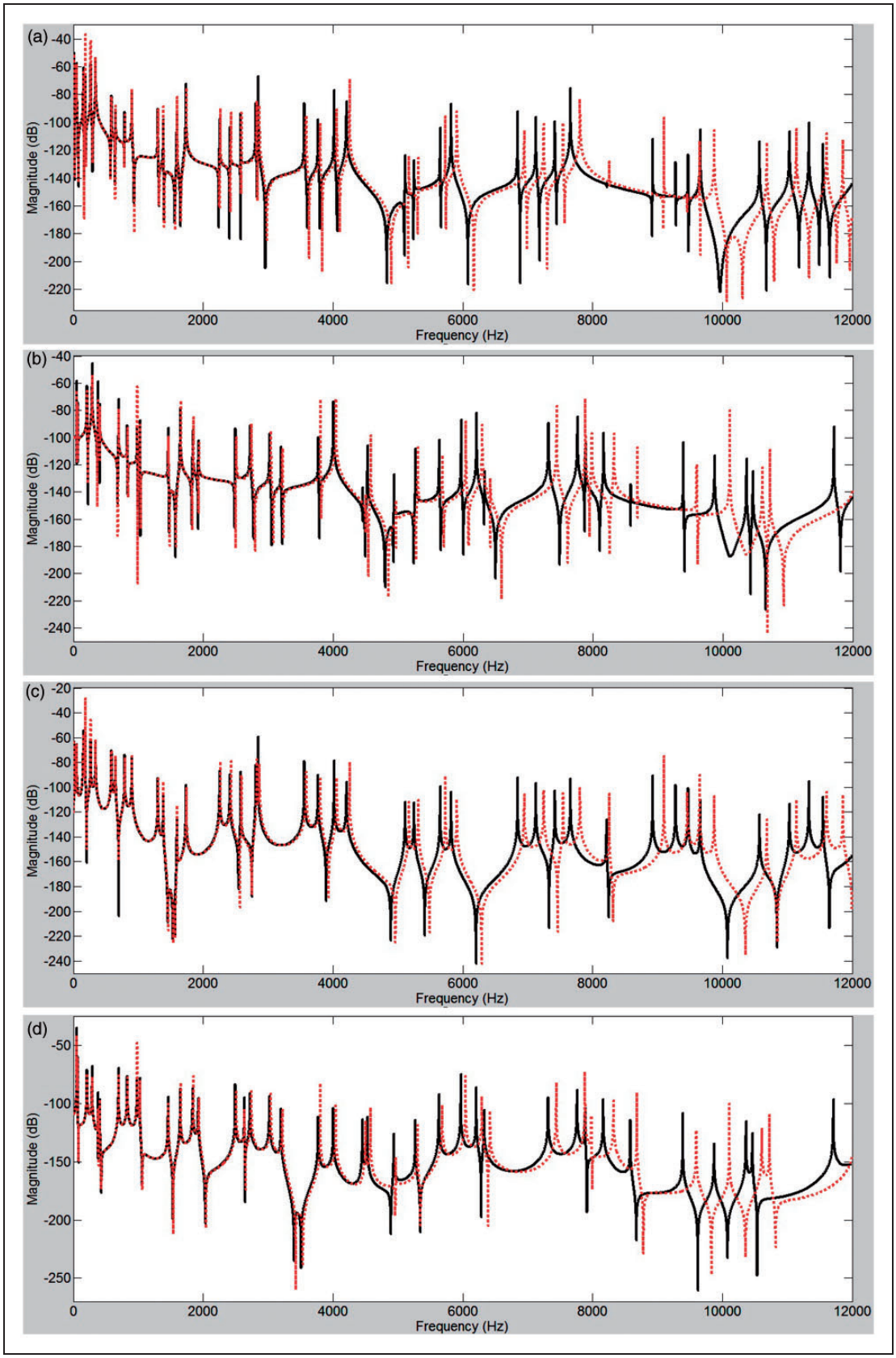

Figure 6. Receptance frequency responses subject to point transverse force excitation: Timoshenko (___) and Euler-Bernoulli (...) bending theories (a) Vertical leg, anti-symmetrical modes, (b) vertical leg, symmetrical modes, (c) horizontal bar, anti-symmetrical modes, (d) horizontal bar, symmetrical modes.

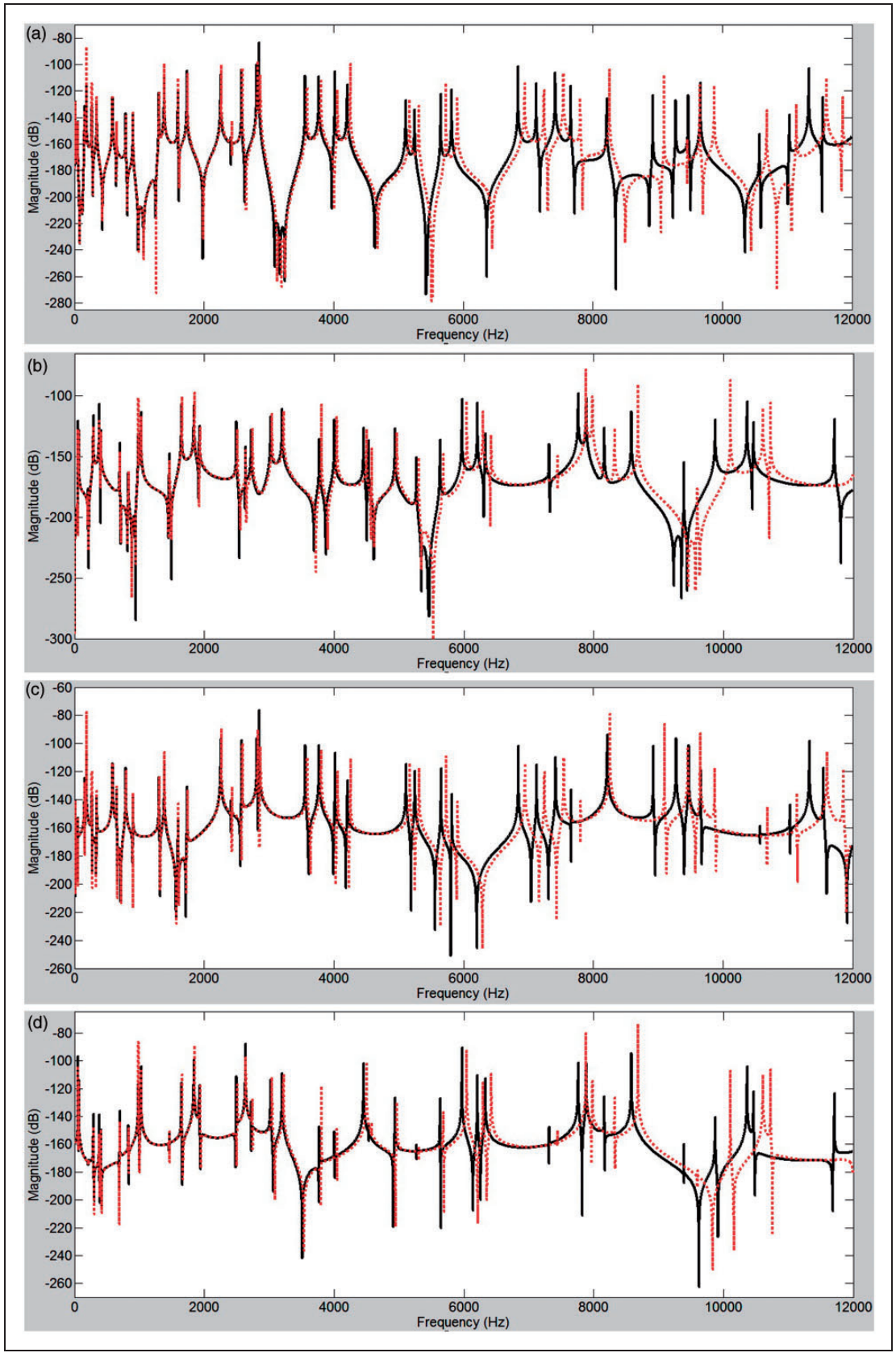

Figure 7. Receptance frequency responses subject to point axial force excitation: Timoshenko (___) and Euler-Bernoulli (...) bending theories (a) Vertical leg, anti-symmetrical modes, (b) vertical leg, symmetrical modes, (c) horizontal bar, anti-symmetrical modes, (d) horizontal bar, symmetrical modes.

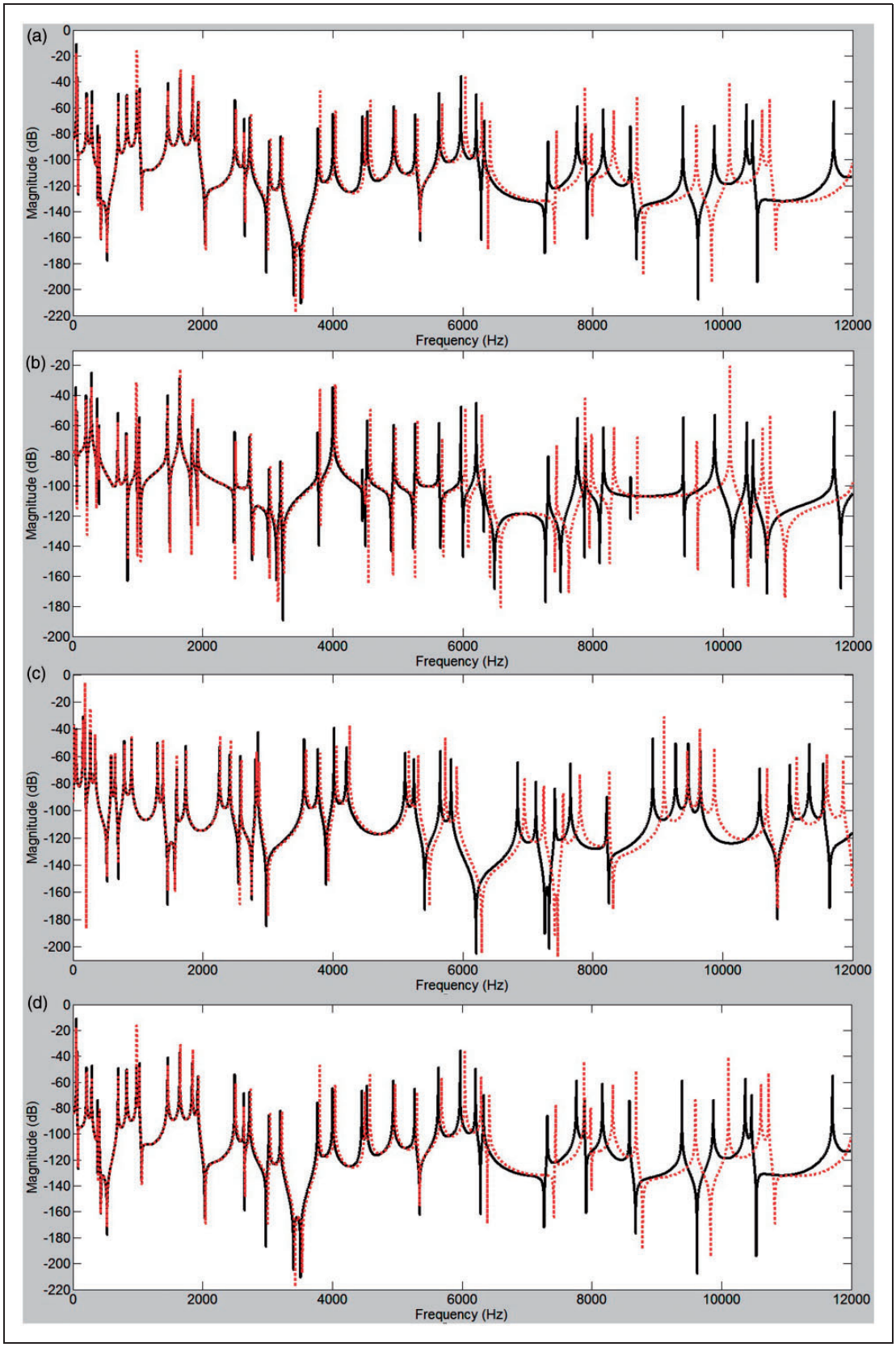

Figure 8. Receptance frequency responses subject to bending moment excitation: Timoshenko (___) and Euler-Bernoulli (...) bending theories (a) Vertical leg, anti-symmetrical modes, (b) vertical leg, symmetrical modes, (c) horizontal bar, anti-symmetrical modes, (d) horizontal bar, symmetrical modes.

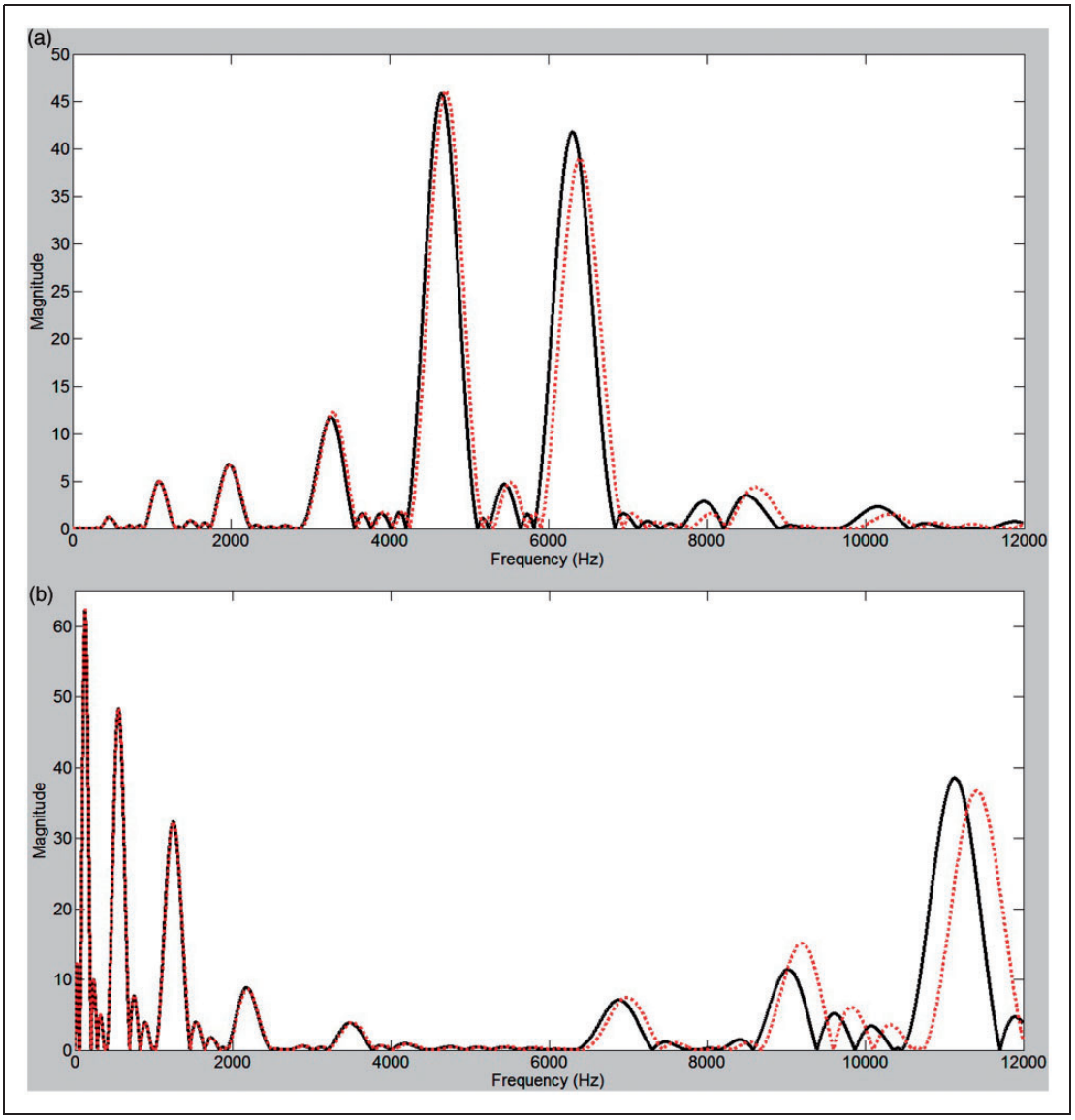

Figure 9. Magnitude responses of characteristic polynomials based on Timoshenko (___) and Euler-Bernoulli (. . .) bending theories: (a) anti-symmetrical modes and (b) symmetrical modes of vibrations.

reflected bending and longitudinal vibration energies. Figure 12 shows the receptance frequency responses of the frame before and after control.

From the above studies, it can be seen that both the feedback wave element and joint control are able to suppress vibrations in a multi-story frame structure effectively. The vibration modes are damped in a broad frequency band, the resonant peaks are much less sharp as a result.

In a practical implementation, the causality (Bruel and Kjael Technical Review, 1984; Pandey, 1995) of a controller must be guaranteed. A causal controller that is an approximation to the ideal controller must be found. One way of finding an approximate causal controller in a digital implementation is to truncate the noncausal part of the ideal controller. Another way is to tune the controller to be optimal at a certain frequency ω_d. The controller given by equation (24a) is purely imaginary and frequency dependent. It is therefore noncausal. This noncausal controller can be tuned to be optimal at ω_d, the control gain then becomes a constant

$$C(\omega_d) = \frac{2GA\kappa[-k_1(\omega_d)N(\omega_d) + k_2(\omega_d)P(\omega_d)]}{\omega_d\sqrt{P(\omega_d)^2 + N(\omega_d)^2}}$$

which is guaranteed to be causal. Recall the receptance frequency responses presented in Figure 10, in which K_R is set to zero, and K_{T1} and

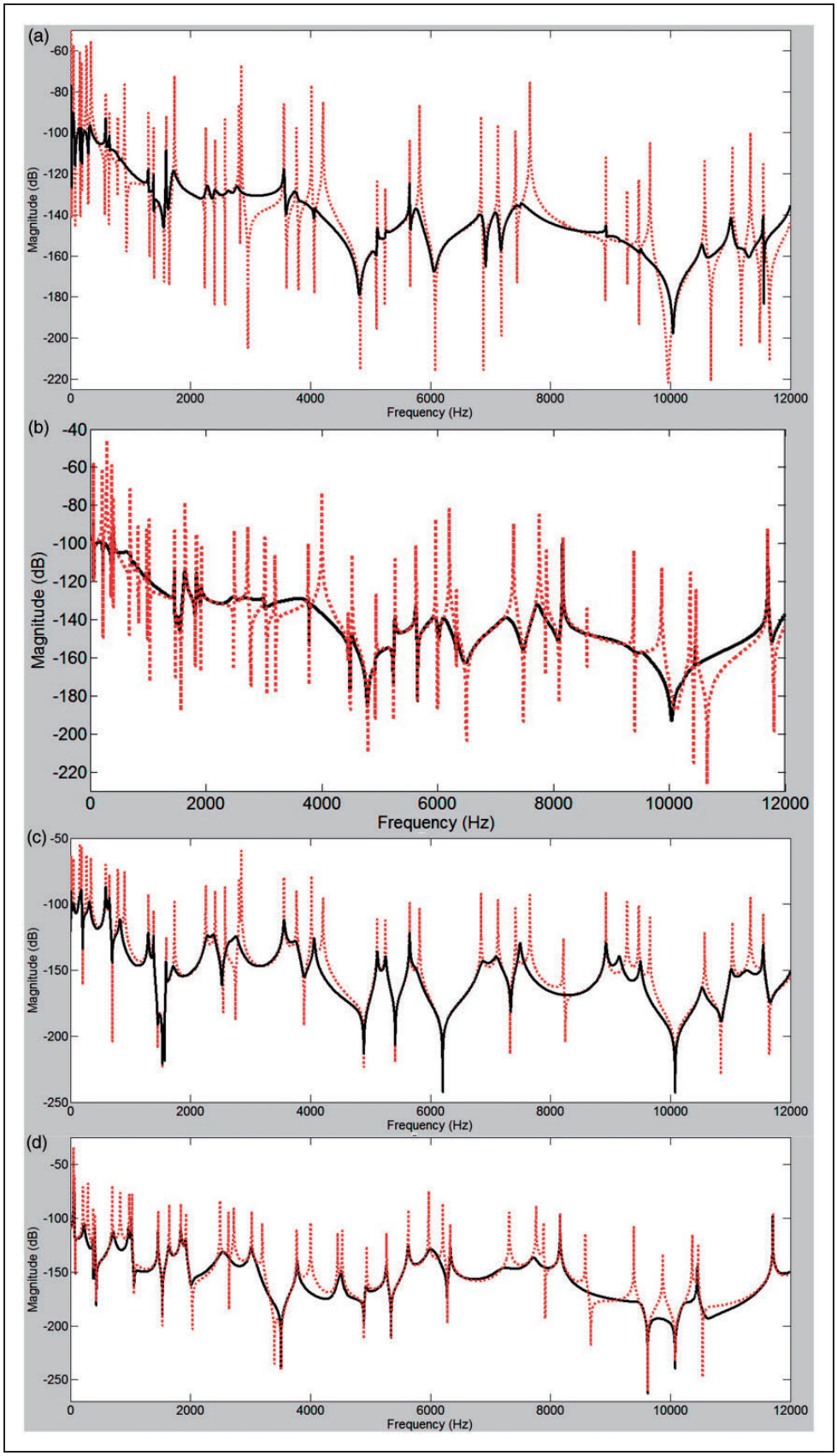

Figure 10. Receptance frequency responses of the multi-story frame: before (...) and after (___) structural element control (a) Vertical leg, anti-symmetrical modes, (b) vertical leg, symmetrical modes, (c) horizontal bar, anti-symmetrical modes, (d) horizontal bar, symmetrical modes.

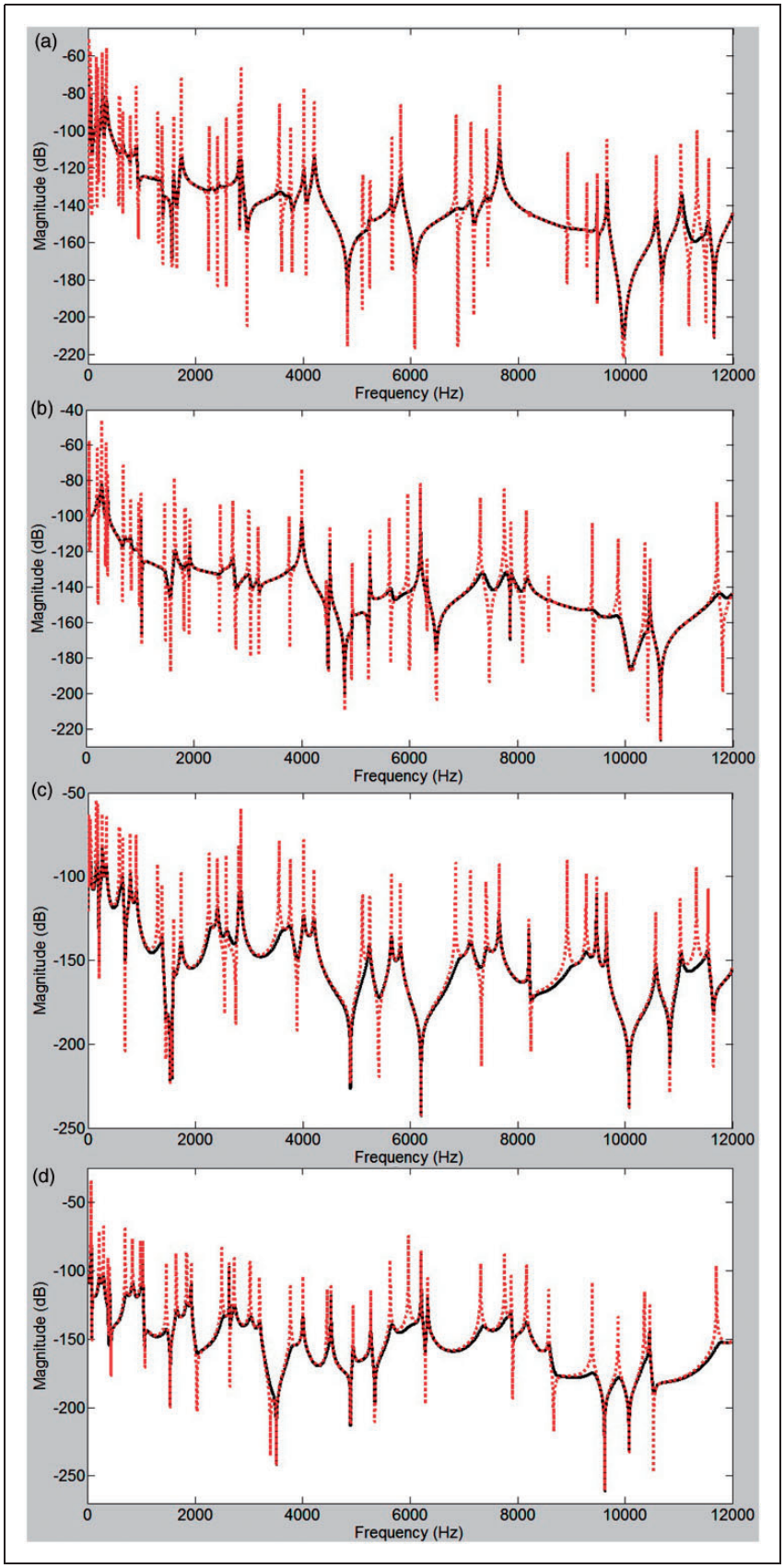

Figure 11. Receptance frequency responses of the multi-story frame: before (...) and after (___) L-joint control (a) Vertical leg, anti-symmetrical modes, (b) vertical leg, symmetrical modes, (c) horizontal bar, anti-symmetrical modes, (d) horizontal bar, symmetrical modes.

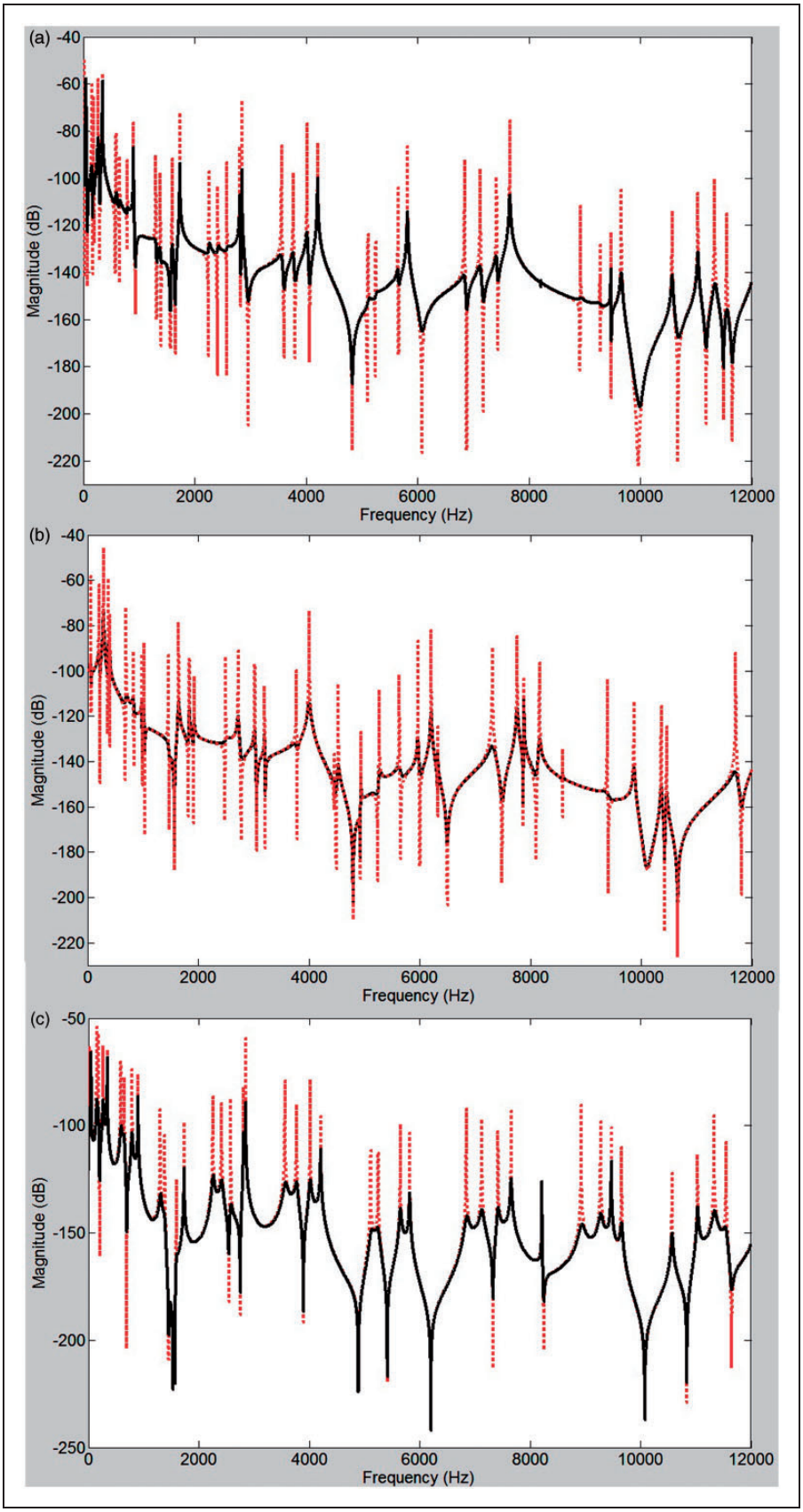

Figure 12. Receptance frequency responses of the multi-story frame: before (...) and after (___) T-joint control (a) Vertical leg, anti-symmetrical modes, (b) vertical leg, symmetrical modes, (c) horizontal bar, anti-symmetrical modes, (d) horizontal bar, symmetrical modes.

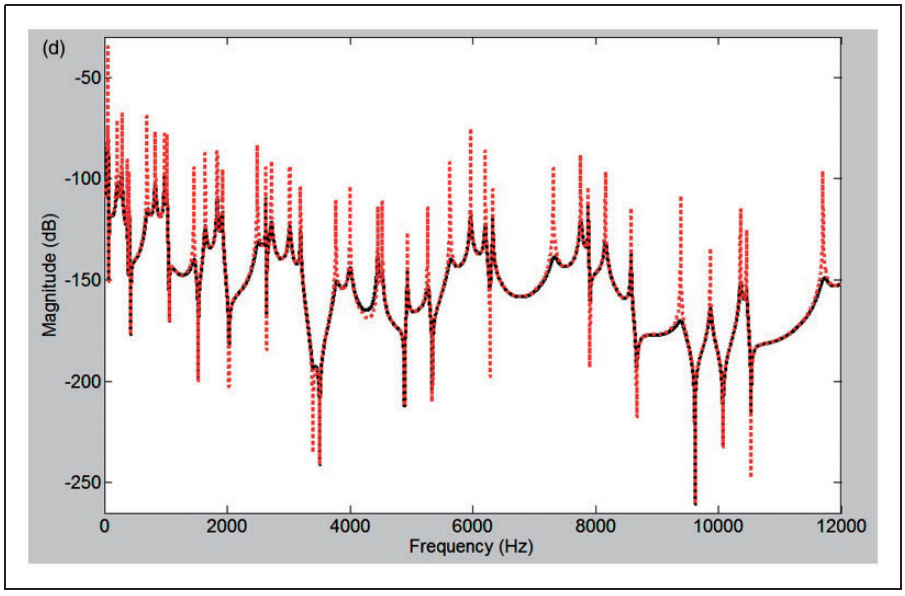

Figure 12. Continued.

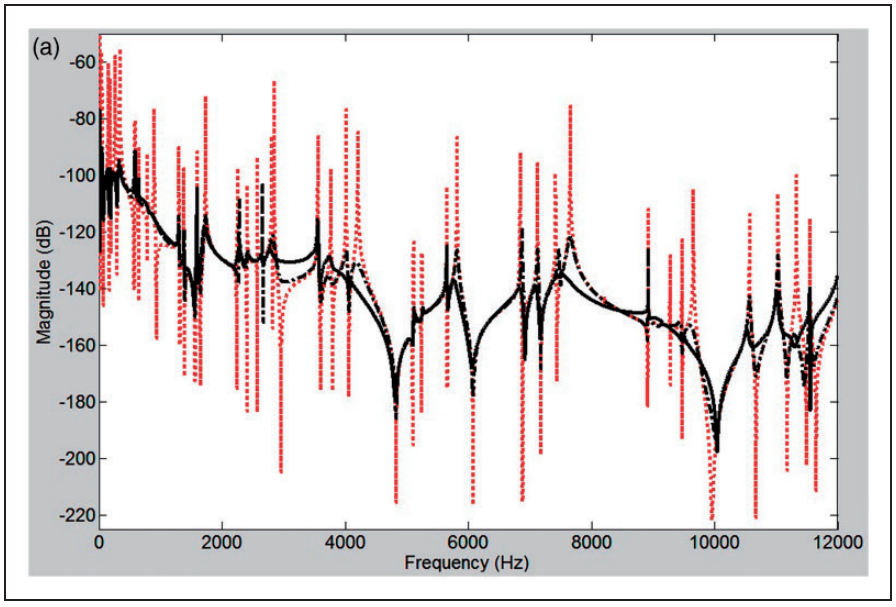

Figure 13. Receptance frequency responses of the multi-story frame: before (. . .), after ideal (___), and after tuned (-.-.-.) structural element control (a) Vertical leg, anti-symmetrical modes, (b) vertical leg, symmetrical modes, (c) horizontal bar, anti-symmetrical modes, (d) horizontal bar, symmetrical modes.

K_{T2} are designed to optimally damp out the flexural and longitudinal vibration energies, respectively. Tuning the noncausal controller K_{T1} to a causal 'D' controller in the form of

$$i\omega \frac{2GA\kappa[-k_1(\omega_d)N(\omega_d)+k_2(\omega_d)P(\omega_d)]}{\omega_d\sqrt{P(\omega_d)^2+N(\omega_d)^2}}$$

allows the controller to be implemented using a viscous damper with damping constant

$$\frac{2GA\kappa[-k_1(\omega_d)N(\omega_d)+k_2(\omega_d)P(\omega_d)]}{\omega_d\sqrt{P(\omega_d)^2+N(\omega_d)^2}}$$

Figure 13 shows the receptance frequency responses of the frame before structural element control, after ideal structural element control, and after tuned

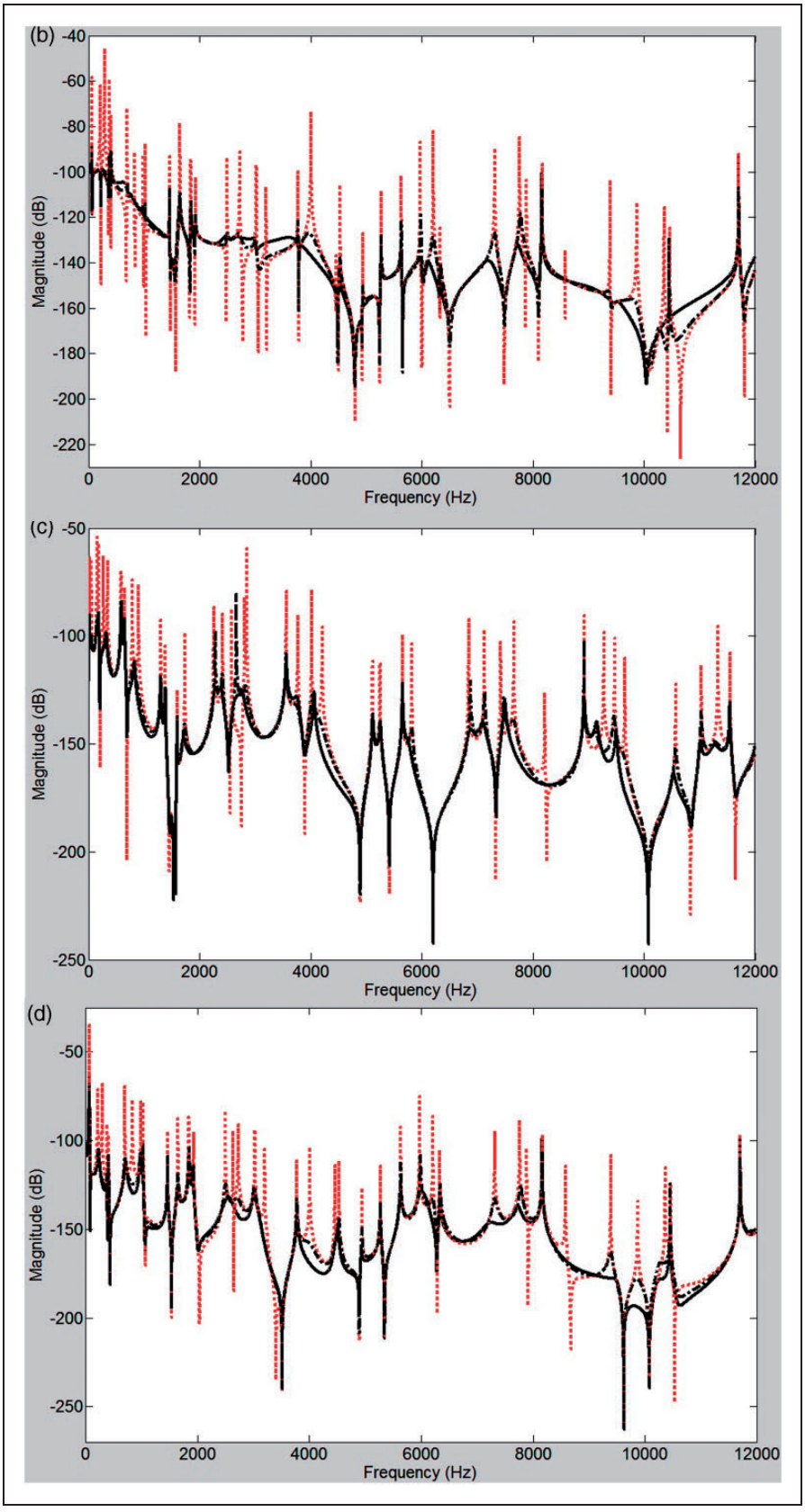

Figure 13. Continued.

structural element control in which the causal bending controller is tuned optimal at 200 Hz. It can be seen that the control performance of the tuned causal controller is the same as that of the ideal controller at the tuned optimal frequency ω_d. The control performance at other frequencies is slightly compromised compared to that of the ideal controller. However, the tuned controller still works very well in damping out the vibration resonances in the broad frequency band.

6. Conclusions

Active wave control was designed based on advanced Timoshenko bending theory to suppress vibrations in a multi-story planar frame structure. Since from a wave point of view, a structure consists of only two basic types of structural components, namely, joints and structural elements, controllers are designed both along structural elements and at structural joints. Feedback wave control strategies such as adding optimal damping to the structure and maximizing the energy absorbed by the controller are considered. Numerical results show that these wave controllers are quite effective in suppressing coupled bending and axial vibrations in complex planar frame structures in a broad frequency band.

This study highlights the fact that at higher frequencies, typically, when the transverse dimensions are not negligible with respect to the wavelength, the effects of rotary inertia and shear distortion can no longer be neglected. In other words, the Timoshenko rather than Euler–Bernoulli beam model must be adopted, for both vibration analysis and control.

Acknowledgements

The author would also like to thank the University of Michigan for providing the Flux high-performance computing system.

Funding

This work was supported by the Civil, Mechanical and Manufacturing Innovation Division of the National Science Foundation (grant no. 0825761).

References

Bishop RED and Johnson DC (1960) *The Mechanics of Vibration*. Cambridge: Cambridge University Press.

Brennan MJ (1994) *Active control of waves on one-dimensional structure*. PhD Thesis, University of Southampton, UK.

Clark RL, Pan J and Hansen CH (1992) An experimental study of the active control of multiple-wave types in an elastic beam. *Journal of Acoustic Society of America* 92(2): 871–876.

Cowper GR (1966) The shear coefficient in Timoshenko's beam theory. *Journal of Applied Mechanics* 33: 335–340.

Cremer L, Heckl M and Ungar EE (1987) *Structure-Borne Sound*. Berlin: Springer-Verlag.

Doyle JF (1989) *Wave Propagation in Structures*. New York: Spring-Verlag.

Elliott SJ and Billet L (1993) Adaptive control of flexural waves propagating in a beam. *Journal of Sound and Vibration* 163(2): 295–310.

Elliott SJ, Brennan MJ and Pinnington RJ (1993) Feedback control of flexural waves on a beam. In: *Proceedings of inter-noise 93*, Leuven, Belgium. pp. 843–846.

Fuller CR, Gibbs GP and Silcox RJ (1990) Simultaneous active control of flexural and extensional waves in beams. *Journal of Intelligence, Material, System and Structure* 1: 235–247.

Gardonio P and Elliott SJ (1995) Active control of multiple waves propagating on a one-dimensional system with a scattering termination. *Active* 95: 115–126.

Ginsberg JH (2001) *Mechanical and Structural Vibrations*. New York: John Wiley and Sons, Inc.

Gladwell GML (1964) The vibration of frames. *Journal of Sound and Vibration* 4: 402–465.

Graff KF (1975) *Wave Motion in Elastic Solids*. Ohio State University Press.

Lu J, Crocker MJ and Raju PK (1989) Active vibration control using wave control concepts. *Journal of Sound and Vibration* 134(2): 364–368.

Mace BR (1987) Active control of flexural vibrations. *Journal of Sound and Vibration* 114(2): 253–270.

Mace BR and Jones RW (1996) Feedback control of flexural waves in beams. *Journal of Structural Control* 3(1–2): 89–98.

Mei C (2002) The analysis and control of longitudinal vibrations from wave viewpoint. *ASME Journal of Vibration and Acoustics* 124: 645–649.

Mei C (2008) Wave analysis of in-plane vibrations of H- and T-shaped planar frame structures. *ASME Journal of Vibration and Acoustics* 130: 061004.

Mei C (2009) Hybrid wave/mode active vibration control of bending vibrations in beams based on advanced Timoshenko theory. *Journal of Sound and Vibration* 322(1–2): 29–38.

Mei C (2011) Wave control of vibrations in multi-story planar frame structures based on classical vibration theories. *Journal of Sound and Vibration* 330: 5530–5544.

Mei C, Mace BR and Jones RW (2001) Hybrid wave/mode active vibration control. *Journal of Sound and Vibration* 247(5): 765–784.

Pandey JN (1995) *The Hilbert Transform of Schwartz Distribution and Applications*. New York: John Wiley and Sons, Inc.

Petyt M (1990) *Introduction to Finite Element Vibration Analysis*. Cambridge: Cambridge University Press.

Rayleigh L (1926) *Theory of Sound*. New York: The Macmillan Company.

Technical Review (1984) *Hilbert Transform*. No. 3, Bruel and Kjael.

Timoshenko SP (1921) On the correction for shear of the differential equation for transverse vibrations of prismatic bars. *Philosophical Magazine* 41(6): 744–746.

Timoshenko SP (1922) On the transverse vibrations of bars of uniform cross sections. *Philosophical Magazine* 43(6): 125–131.

Vipperman JS, Burdisso RA and Fuller CR (1993) Active control of broadband structural vibration using the LMS adaptive algorithm. *Journal of Sound and Vibration* 166(2): 283–299.

Von Flotow AH (1985) Traveling wave control for large spacecraft structures. *Journal of Guidance* 9(4): 462–468.

Wang CH and Rose LRF (2003) Wave reflection and transmission in beams containing delamination and inhomogeneity. *Journal of Sound and Vibration* 264: 851–872.